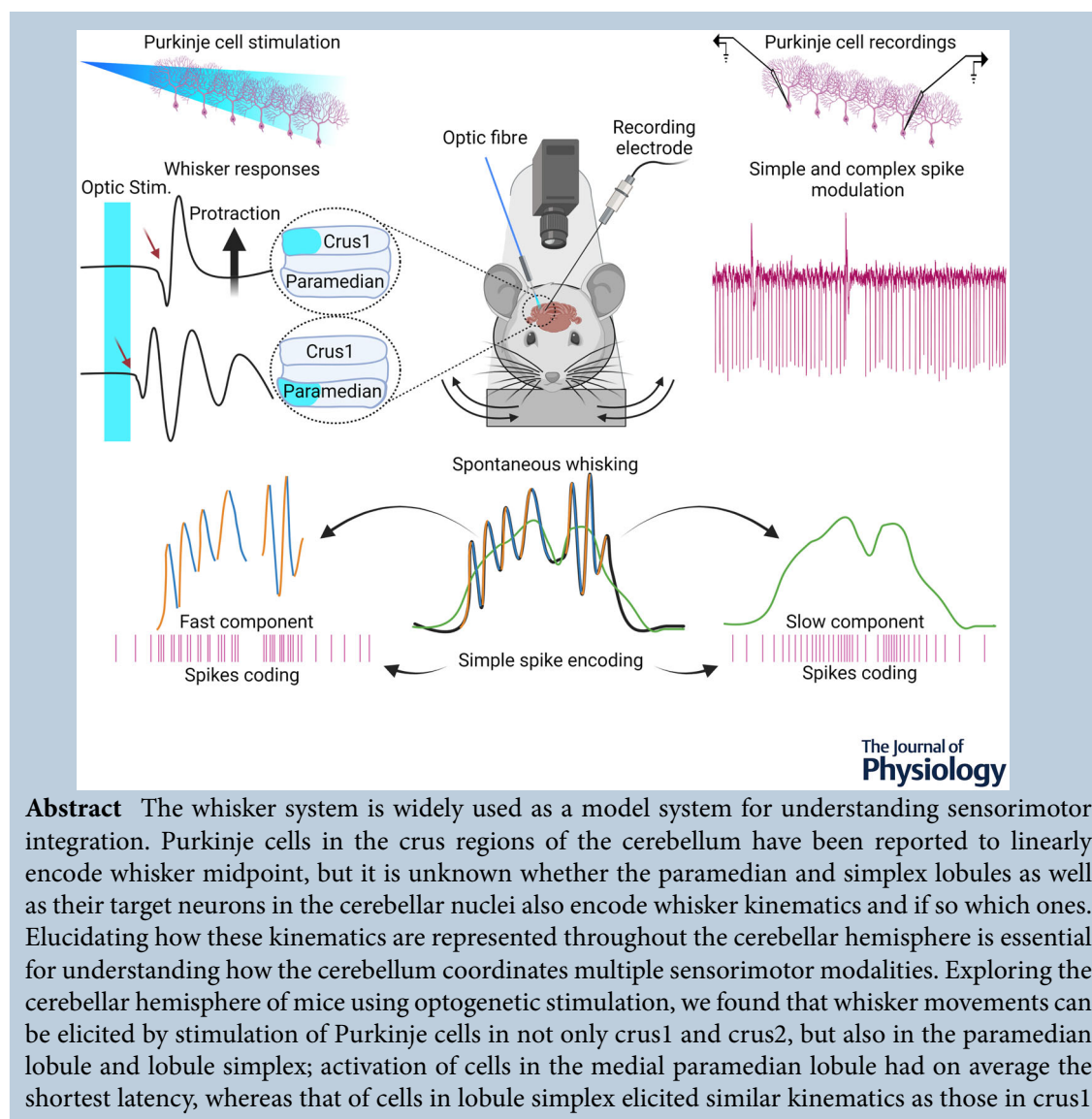# Whisker kinematics in the cerebellum

Peipei Zhai[1] , Vincenzo Romano[1] , Giulia Soggia[1] , Staf Bauer[1] , Nathalie van Wingerden[1],
Thomas Jacobs[1] , Annabel van der Horst[1] , Joshua J. White[1], Roberta Mazza[1] and Chris I. De Zeeuw[1,2]

[1] *Department of Neuroscience, Erasmus MC, Rotterdam, Netherlands*
[2] *Netherlands Institute for Neuroscience, Royal Dutch Academy of Arts & Sciences, Amsterdam, Netherlands*

Handling Editor: David Wyllie

The peer review history is available in the Supporting Information section of this article (https://doi.org/10.1113/JP284064#support-information-section).

The Journal of Physiology

Abstract The whisker system is widely used as a model system for understanding sensorimotor integration. Purkinje cells in the crus regions of the cerebellum have been reported to linearly encode whisker midpoint, but it is unknown whether the paramedian and simplex lobules as well as their target neurons in the cerebellar nuclei also encode whisker kinematics and if so which ones. Elucidating how these kinematics are represented throughout the cerebellar hemisphere is essential for understanding how the cerebellum coordinates multiple sensorimotor modalities. Exploring the cerebellar hemisphere of mice using optogenetic stimulation, we found that whisker movements can be elicited by stimulation of Purkinje cells in not only crus1 and crus2, but also in the paramedian lobule and lobule simplex; activation of cells in the medial paramedian lobule had on average the shortest latency, whereas that of cells in lobule simplex elicited similar kinematics as those in crus1

P. Zhai and V. Romano contributed equally to this work.

and crus2. During spontaneous whisking behaviour, simple spike activity correlated in general better with velocity than position of the whiskers, but it varied between protraction and retraction as well as per lobule. The cerebellar nuclei neurons targeted by the Purkinje cells showed similar activity patterns characterized by a wide variety of kinematic signals, yet with a dominance for velocity. Taken together, our data indicate that whisker movements are much more prominently and diversely represented in the cerebellar cortex and nuclei than assumed, highlighting the rich repertoire of cerebellar control in the kinematics of movements that can be engaged during coordination.

Corresponding author Vincenzo Romano: Department of Neuroscience, Erasmus MC, Rotterdam, Netherlands. Email: v.romano@erasmusmc.nl

Abstract figure legend We optogenetically stimulated Purkinje cells (PCs) in various cerebellar lobules, while recording their activity and monitoring whisker kinematics. Excitation of PCs throughout the cerebellar hemispheres induced whisker movement, with the shortest latency and longest duration within the paramedian lobe. During spontaneous whisking behaviour, simple spike activity encoded whisker kinematics at different time scales showing a stronger correlation with velocity than with position.

Key points

- Excitation of Purkinje cells throughout the cerebellar hemispheres induces whisker movement, with the shortest latency and longest duration within the paramedian lobe.
- Purkinje cells have differential encoding for the fast and slow components of whisking.
- Purkinje cells encode not only the position but also the velocity of whiskers.
- Purkinje cells with high sensitivity for whisker velocity are preferentially located in the medial part of lobule simplex, crus1 and lateral paramedian.
- In the downstream cerebellar nuclei, neurons with high sensitivity for whisker velocity are located at the intersection between the medial and interposed nucleus.

Introduction

The whisker system is a widely used model to unravel how the brain controls sensorimotor behaviour (Auffret et al., 2018; Crochet et al., 2011; Hill et al., 2011; Lang et al., 2006; Lindeman et al., 2021; O'Connor et al., 2002; Takatoh et al., 2022). While collecting sensory information, rodents rhythmically protract and retract their whiskers to actively explore the environment (Kleinfeld et al., 2006; Prescott et al., 2011). Such whisking behaviour requires optimal motor actions at multiple time scales to properly examine the sensory world (Hill et al., 2011). The dynamic coordination of triphasic neuromuscular activity generates various whisker movement components, which have been described as phase, midpoint and amplitude of the envelope (Hill et al., 2008; Sreenivasan et al., 2016) or velocity and amplitude of protractions and retractions (Towal & Hartmann, 2008).

Peipei Zhai is a 4th-year PhD student in the neuroscience department of Erasmus Medical Centre, supervised by Professor Chris de Zeeuw. Her doctoral research focuses on investigating the role of the cerebellum in whisking movements. Specifically, she is studying the activity patterns and mechanisms involved in the cerebellar control of whisker movements. She holds a bachelor's degree in clinical medicine and a master's degree in neurology, both obtained from Nantong University in China. Her educational background in these fields provides her with a solid foundation for her current research in neuroscience. Her research is supported by the China Scholarship Council. **Vincenzo Romano** is a goal-oriented, passionate researcher with 10 years of experience in system physiology. He started his career at the University of Pavia in the lab of Professor Egidio D'Angelo and later joined the group led by Professor Chris De Zeeuw in Rotterdam. He studied how the cerebellum allows us to learn to react faster to external stimuli, how we coordinate body movement with respiration and which signals coordinate the left and right part of the body. Currently he is a team-leader aiming to elucidate how cerebro-cerebellar communication coordinates the complex movement of the entire body.

While activity of the intrinsic muscles directly affects the velocity of the whisker movements at each cycle, that of the extrinsic muscles largely determines their midpoint (Bellavance et al., 2017; Hill et al., 2008).

Coordination of the different whisker movement components during active exploration requires communication between a complex network of different brain areas (Bosman et al., 2011). Among these areas is the cerebellum, which receives and sends signals related to whisker kinematics from and to several areas of the brainstem and cerebrum. The sensory information from the whiskers relayed to the cerebellar cortex via the mossy fibre and climbing fibre system has been described for crus1 and crus2, revealing a fractured somatotopic organization (Bosman et al., 2010; Bosman et al., 2011; Brown & Raman, 2018; Romano et al., 2018; Shambes et al., 1978). Accordingly, Purkinje cell (PC) activity of these crus regions has been shown to modify and encode whisker motion (Bosman et al., 2010; Bosman et al., 2011; Brown & Raman, 2018; Chen et al., 2016; Proville et al., 2014; Romano et al., 2018; Romano et al., 2022). Indeed, the kinematics of whisking may be coordinated by modulations of both simple spikes (SSs) and complex spikes (CSs), which are evoked by changes in the mossy fibre and climbing fibre pathway, respectively (De Zeeuw et al., 2011; Romano et al., 2022; Thach, 1968). For example, SS activity of PCs in crus1 has been reported to linearly encode the position of the slow component of spontaneous whisker movements, including the whisker midpoint or setpoint (Chen et al., 2016). However, whether the same and/or a different group of PCs also encodes different time scales such as the fast component of individual protractions and retraction is still unknown.

To date, it has been shown for many other types of movements, such as compensatory and saccadic eye movements as well as limb and eyeblink movements, that the SS modulation of PCs often carries a strong and dominant velocity signal (De Zeeuw et al., 1995; Herzfeld et al., 2015; Hewitt et al., 2011; Muzzu et al., 2018; Sauerbrei et al., 2015; ten Brinke et al., 2015). To further advance our understanding of the cerebellar contribution in the coordination of whisker movements, we set out to investigate to what extent PCs in lobules other than the crus regions, such as the neighbouring paramedian lobule and lobule simplex, are also involved in coordinating whisker movements, and to what extent PCs in the cerebellar cortex and their target neurons in the cerebellar nuclei (CN) (De Zeeuw & Berrebi, 1995) also encode velocity signals. To address these questions, we optogenetically stimulated PCs in the paramedian lobule and lobule simplex in awake head-fixed mice while recording their whisker movements, and we compared the kinematics of these responses with those obtained by stimulating crus1 and crus2. Moreover, to uncover the SS and CS encodings in these regions, we also extracellularly recorded PC activity and examined their relationship to the different kinematic components of whisker movements during voluntary spontaneous behaviour. Finally, we recorded neural activity in the CN to explore which kinematic parameters are encoded downstream of the PCs and to determine to what extent these encodings are preserved within the same PC–CN microcomplex (Beekhof et al., 2021; De Zeeuw, 2021). Our results highlight that PCs in both the paramedian lobule and lobule simplex may play prominent and versatile roles in the coordination of whisker movements, adding to the contributions provided by PCs in crus1 and crus2. Moreover, analysis of PC activity in all four tested lobules, as well as that of their CN target neurons, highlights that velocity is the most dominant kinematic parameter encoded in the cerebellum.

Methods

Mice

All mice experiments were done according to the Animals guidelines of the institutional animal welfare committee of Erasmus MC by the Central Authority for Scientific Procedures. Wild-type C57BL/6J (No. 000664) and transgenic L7-Ai27D (No. 012567) mice were obtained from the Jackson Laboratory (Bar Harbor, ME, USA). Mice aged 6–34 weeks were used in this study and the mice were housed individually in a 12 h light–dark cycle with food and water available *ad libitum*. The ambient housing temperature was maintained at ∼25.5°C with 40–60% humidity. We used 19 mice for the optogenetic stimulation experiments and 53 mice for the recordings of 233 PCs and 78 CN neurons. After the experiment mice were killed by cervical dislocation.

Surgeries

For all mice, a magnetic pedestal was placed on the skull above the bregma using Super-Bond C&B (Sun Medical, Furutaka-cho, Japan) and a craniotomy was made over the right hemisphere of the cerebellum. Isoflurane anaesthesia (Pharmachemie, Haarlem, The Netherlands; 2–4% v/v in O_2) was maintained during the whole surgery procedure. Mice were given 5 mg/kg carprofen ('Rimadyl', Pfizer, New York, USA), 50 μg/kg buprenorphine ('Temgesic', Reckitt Benckiser Pharmaceuticals, Slough, UK), 1 μg lidocaine (AstraZeneca, Zoetermeer, The Netherlands) and 1 μg bupivacaine (Actavis, Parsippany-Troy Hills, NJ, USA) to reduce postsurgical pain. After 48 h of recovery, mice were habituated to the recording apparatus for about 45 min during at least two daily sessions. In the recording apparatus, mice were head-fixed with the pedestal and restrained.

Whisker tracking

The whisker movements were tracked as described previously (Romano et al., 2020) using the BIOTACT Whisker Tracking Tool (Perkon et al., 2011) in combination with custom-written code (https://github.com/elifesciences-publications/BWTT_PP). The whisker movements were described as the average angle of all trackable whiskers per frame.

Electrophysiology and spike sorting

Electrophysiological recordings were performed as described previously (Romano et al., 2022) in awake mice using quartz-coated platinum/tungsten electrodes (2–5 MΩ, outer diameter 80 μm, Thomas Recording, Giessen, Germany) placed in an 8 × 4 matrix (Thomas Recording), with an interelectrode distance of 305 μm. Before recording, we removed the dura of the opened hemisphere, fixed the mice in the apparatus and adjusted all manipulators under light anaesthetization with isoflurane. Recordings began at least 30 min after turning off the anaesthesia and in the right hemisphere at a minimal depth of 500 μm. The electrophysiological signal was digitized at 25 kHz, using a 1 to 6000 Hz band-pass filter, 22× pre-amplified, and stored using an RZ2 multichannel workstation (Tucker-Davis Technologies, Alachua, FL, USA). Spikes were detected offline using SpikeTrain (Neurasmus, Rotterdam, The Netherlands) as we previously described (Romano et al., 2018; Romano et al., 2020; Romano et al., 2022). The PC signal was recognized by the appearance of the typical CS and SS. The criterion for a single PC recording was the minimal interspike interval of SSs was of 3 ms and each CS was followed by a pause in SS firing of at least 8 ms. A recording was considered to originate from a CN neuron based on stereotaxic coordinates and *post hoc* electrolytic lesions made in a subset of experiments. To avoid the firing rate change being due to instability of the recording, we excluded recordings in which the amplitude or the width of more than three consecutive SSs exceeded three standard deviations above or below their average. Only those recordings during which the amplitude and the width of the spikes were constant over time were included in our study. When these criteria were satisfied, we considered them stable single-unit recordings of PCs. In total 233 PCs and 78 CN cells fulfilled these criteria. Often multiple cells were recorded simultaneously from the same mouse.
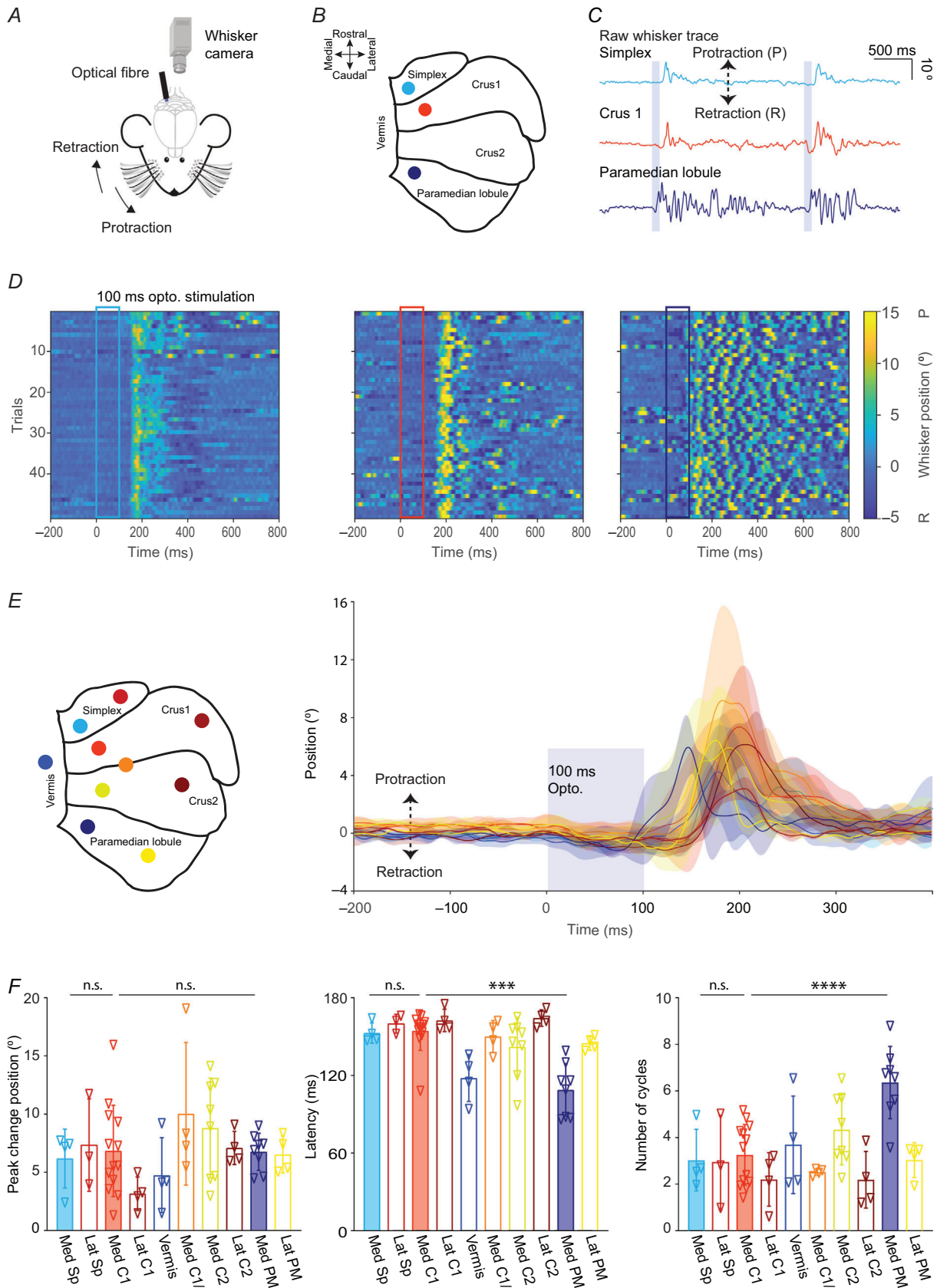
Optogenetic stimulation

Only transgenic L7-Ai27D mice expressing channelrhodopsin-2 specifically in PCs were used for these experiments. LED photostimulation (wavelength = 470 nm, M470F3, Thorlabs, Newton, NJ, USA) was given by a high-power light driver (DC2100, Thorlabs) through an optic fibre (400 μm in diameter, Thorlabs). The optic fibre was placed on the surface of the right cerebellar hemisphere in 10 different locations. The stimulation lasted 100 ms in 2 s intervals. The intensities of the light stimulation varied from 1 to 10 mW. As in Romano et al. (2022), the intensity was calibrated so that only whisker movements were triggered when the mouse was at rest. This was done by reducing the light intensity when eye or front paw movement was induced by the stimulation. This, together with the relatively short latency (∼20 ms after the stimulus offset), allowed us to exclude the possibility that whisker movements were reflecting largely secondary effects following other non-whisking movements. PC excitation was unlikely to induce a startle response, because a sequence of relatively short stimuli (20 ms) entrains rather than attenuates whisker movements (Bauer et al., 2022), as would be expected by a prepulse inhibition effect. Using a 400 μm diameter fibre resulted in an irradiation of 8–80 mW/mm. Based on the calculation reported by Chaumont et al. (2013), we estimated that the light stimulation could activate 1000/6000 PCs. Because this is not an accurate numerical prediction and might differ greatly depending on the site of stimulation, we cannot exclude that some PCs could be activated by light delivered in two neighbouring stimulation sites. From a control experiment, we estimated that PCs could be activated by an optic fibre located within ∼1000 μm Euclidian distance (Fig. A1*E*, *F*). From this estimation, of how localized the PC activation was, we can exclude that stimulation of distal locations (e.g. simplex and paramedian lobule which lie ∼2500 μm apart) could activate the same group of PCs.

Statistics and visualization

For Fig. 1, each mouse received different stimulations from the 10 locations (medial simplex: 4 mice; lateral simplex: 3 mice; medial crus1: 13 mice, lateral crus1: 4 mice; medial crus1/2: 4 mice; vermis: 4 mice; medial crus2: 8 mice, lateral crus2: 4 mice; medial paramedian: 8 mice, lateral paramedian: 4 mice). The start of the whisker movement was considered as the time at which the movement exceeded 3 SD ± baseline (from −200 to −100 ms relative to the onset of the stimuli). The latency of the whisker movement was calculated as the time from the onset of stimulation to the start of the movement. Throughout this study, the whisker heatmap was plotted using a custom code based on the MATLAB function 'imagesc'. In Fig. 2*C*, we aligned the whisker kinematics around each SS and calculated its average per PC; in Fig. 2*D*, we performed the same analysis, but aligned the kinematics around each CS; and in Fig. 5*D* we

Figure 1. Optogenetic stimulation of Purkinje cells (PCs) triggers specific patterns of whisker movements depending on the cerebellar area

A, a schematic of the experimental set-up, which includes a high-speed camera for recording whisker movements of a head-fixed mouse and an optical fibre to provide the optogenetic stimulation on top of the cerebellar cortex. *B*, schematic of the dorsal view of the right cerebellar hemisphere showing three examples of sites for optogenetic stimulation; light blue, red and dark blue dots indicate stimulation in medial lobule simplex (SP), medial crus1 (C1) and medial paramedian lobule (PML), respectively. *C*, three example traces of representative profiles of whisker movements upon PC stimulation of the three corresponding sites of stimulation. The purple bars indicate the 100 ms episodes of optogenetic stimulation. Protractions (P) and retractions (R) are represented by upward and downward deflections, respectively. *D*, trials of optogenetically induced whisker movements are shown as heatmap raster plots for stimulations in medial SP (left), C1 (middle) and PML (right) of the same mouse presented in *B* and *C*. Zero represents the stimulation onset, the coloured frames indicate the period of optogenetic stimulation, and each row shows the whisker movements of a single trial. *E*, schematic of all the optogenetic stimulation areas (left). The population average whisker movements (right) for each stimulated area are represented with the colours matching the schematic on the left. The shaded areas above and below the lines representing the averages indicate the standard deviation. The purple shaded column highlights the 100 ms period of optogenetic stimulation. *F*, bar plots showing the amplitude (left), latency (middle) and number of whisking cycles (right) for each of the stimulated cerebellar areas. The latencies were calculated from the profile of the whisker movements starting at stimulation onset. The total amount of induced whisking cycles during the first 1000 ms after stimulus onset. Note that the filled bars indicate the data tested for differences (latency Med C1 *vs.* PM $P = 1.07 \times 10^{-5}$; number of cycles Med C1 *vs.* PM $P = 9.17 \times 10^{-5}$. Error bars indicate the standard deviation. See also Appendix Fig. A1.

aligned the kinematics around each CN neuron spike. We decided to align whisker kinematics around each SS because each SS could induce (or be affected by) small whisker displacement within each whisking cycle. Before extracting protraction and retraction (Towal & Hartmann, 2008), we processed the whisker signal using a 2 Hz high-pass filter to align the whisker baseline to zero. Our aim was not to extract the slow component of the midpoint, which has been previously calculated using a 6 Hz low-pass filter (Chen et al., 2016; Cheung et al., 2019). We have chosen the cut-off frequency of 2 Hz, because under our experimental circumstances rhythmic whisking occurs in the range of 3–30 Hz (Bauer et al., 2022; Cao et al., 2012; Kleinfeld et al., 2016; Moore et al., 2013; Romano et al., 2022), while the slow pad movements have been reported at 1–2 Hz (Bermejo et al., 2005). Individual whisker protractions and retractions in Figs 3, 5 and A3 were detected with custom MATLAB code that detected the maximum and minimum points of the filtered whisker signal (30 Hz low-pass filter). Only segments with amplitude >3 degrees were considered for this analysis. Protractions featuring a succession of two of those segments (i.e. double pumps) were not included (Towal & Hartmann, 2008). The heatmap of anatomical distribution maps in the cerebellum was made similarly to that previously described (Romano et al., 2018; Romano et al., 2020; Romano et al., 2022). The locations of all recorded PCs were attributed to the corresponding position of a rectangular grid (4 × 4) covering the right cerebellar hemispheres. The mean or standard deviation of each parameter on this map was calculated per grid position and interpolated between each grid position and its neighbours. The black lines indicate the borders to the cerebellar zones. For the CN anatomical distribution maps, we attributed the 78 CN cells to a mediolateral CN configuration aligned from 1 to 8. The corresponding parameter on this map was calculated and averaged

similarly to the PCs, per grid position, and subsequently interpolated with its neighbours. For the most extreme lateral portion of the CN, we calculated the mean value of the CN cells in the most extreme position and plotted the interpolated mean value showing a transition from the most extreme lateral part of the schematic to the medial part. In Figs 4, 6 and A4, the individual protractions and retractions were divided into three groups based on amplitude or velocity. After sorting the amplitude of protraction in ascending order, if the amplitude is within the first 1/3 (0–33%) of all the movements, the protraction was placed in the group 'low'. If the amplitude was between 1/3 and 2/3 (33–66%) of all the movements, the protraction was placed in the group 'middle'. If the amplitude was within the last 1/3 (66–100%) of all the movements, the protraction was placed in the group 'high'. We quantified the firing rate modulation (maximal modulation from −50 to 50 ms to the movement onset) when the amplitude of the movements was 'low', 'middle' or 'high' and analysed the difference in firing rate between 'low' and 'high'.

Results

Optogenetic stimulation of Purkinje cells triggers region-specific movement patterns

To investigate whether the paramedian lobule and lobule simplex may also be involved in coordinating whisker movements, we compared the impact of optogenetic stimulation of their PCs with that following stimulation of PCs in crus1 and crus2. In 19 awake, head-fixed L7-Ai27D mice, PCs of the right cerebellar hemisphere were optogenetically stimulated while recording whisker movements (Fig. 1A); this type of stimulation is known to instantly induce an increase in SS activity, because of the expression of channelrhodopsin-2 specifically in
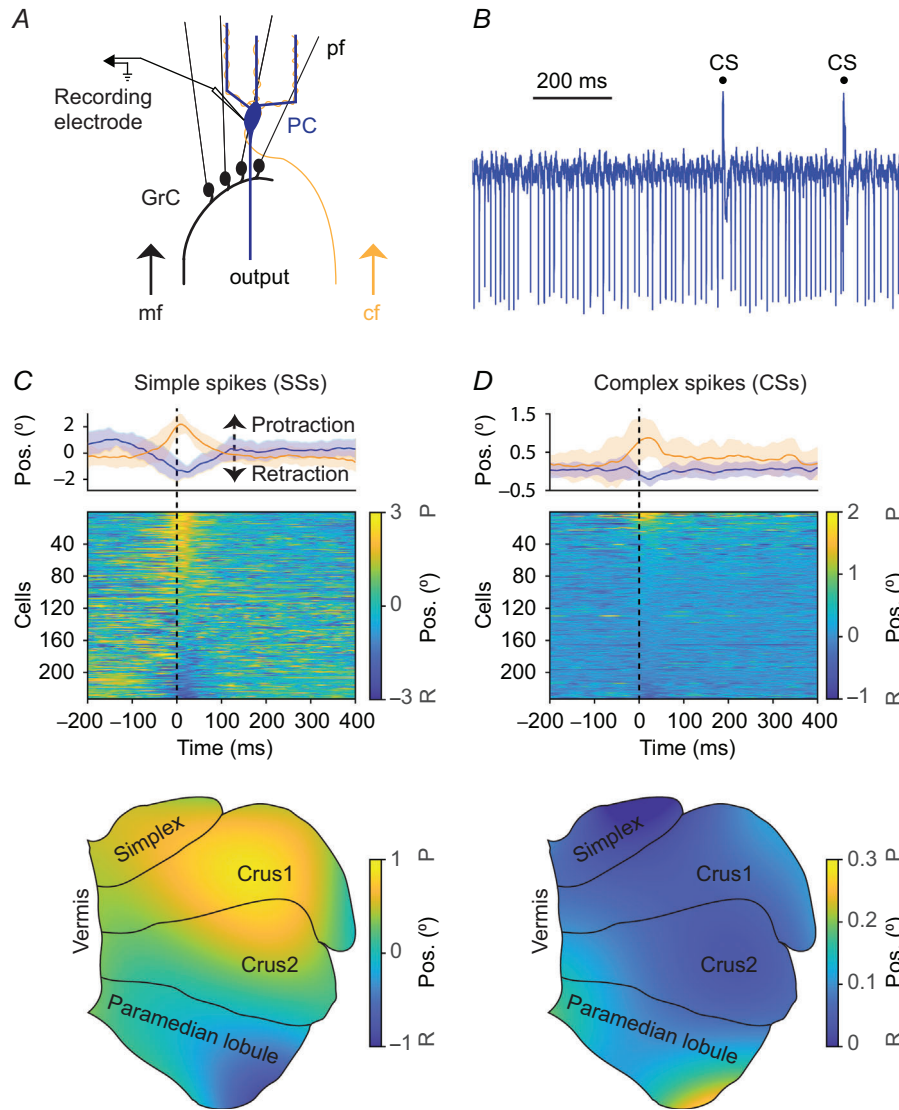
Figure 2. Changes in protraction or retraction of the whiskers aligned to simple spike (SS) and complex spike (CS) activity

A, a schematic of the circuitry of the cerebellar cortex, highlighting a Purkinje cell (PC) that receives input from multiple parallel fibres (pf) as well as a single climbing fibre (cf). The tip of the electrode for recordings is close to the soma of the PC, allowing identification of both the SSs and CSs, which are modulated by the pf and cf input, respectively. Note that parallel fibres originate in the granule cells (GrC), which in turn receive a mossy fibre (mf) input. *B*, an example of the activity of a PC, showing both SSs (downward deflections) and CSs (upward deflections indicated by black dots). *C*, average whisker position around the SS times. The heatmap is composed of 233 lines each representing the change in whisker position around the SS times of each PC (indicated at 0 with the dashed line). Cells are sorted according to the changes in whisker position in the first 50 ms after the SS times. Some PCs have SSs associated with protraction (P, positive values in yellow) and some with retraction (R, negative values in blue). The orange and blue lines above the heatmap represent the average change in whisker position relative to the cells for which the SSs are associated with forward or backward whisker movement, respectively (i.e. *n* = 37 for the PCs with the strongest modulation for protraction; *n* = 37 for the PCs with the strongest modulation for retraction); the shaded areas around the lines represent the standard deviation. The bottom panel shows the distribution of the preferred correlations of these PCs with either protraction or retraction for the 50 ms period after SS across the lobules in the cerebellar hemisphere. *D*, similar to *C*, but for CSs. The distributions of the areas correlating with protraction or retraction are reciprocal for CS and SS activity. Note that the scale bars for the heatmaps are different for *C* and *D*, indicating that larger whisker movements are observed around SSs as compared to CSs. See also Appendix Fig. A2.

A

B

C
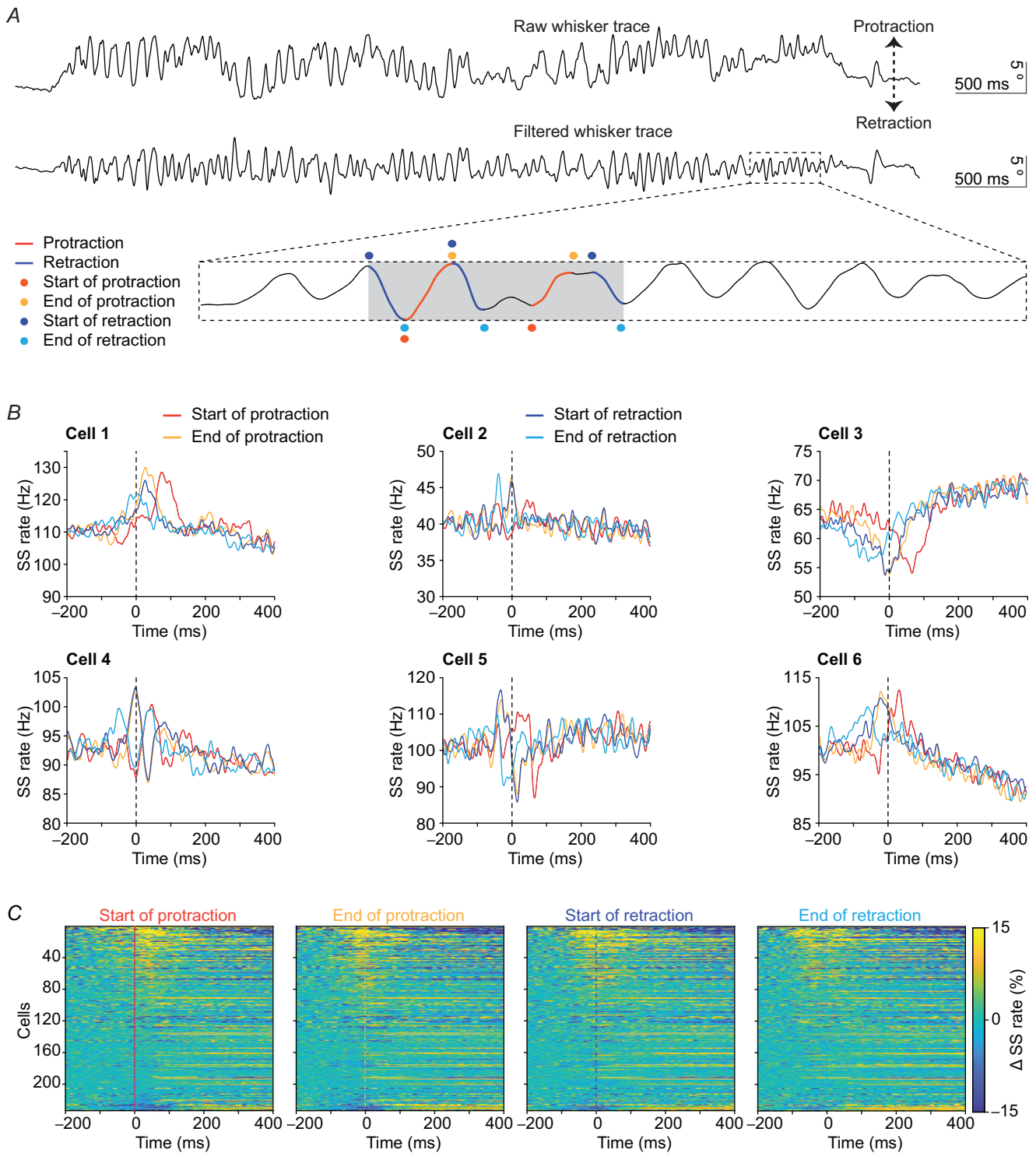
Figure 3. Simple spike (SS) modulations of different PCs differentially encode the beginning and end of spontaneous whisker protractions and retractions

A, example of a whisker movement as a raw (top panel) and high-pass filtered trace (middle panel), with an enlargement for a 500 ms period (bottom panel, corresponding to the inset in the middle panel). Spontaneous whisker movements are characterized by quasiperiodic oscillations consisting of protractions and retractions, the start and endpoint of which are identified and used for further analysis. Dark and light orange dots indicate the start and end of protractions, while dark and light blue dots denote the start and end of retractions, respectively. Dark orange and blue lines indicate protractions and retractions, respectively. *B*, convolved peri-event time histogram (PETH) of SS firing rate for six different example cells in relation to the four whisker movement phases; colour

coding as in *A*. *C*, SS activity of all 233 recorded PCs plotted as heatmaps aligned to the start of protraction (left), end of protraction (left-middle), start of retraction (right-middle) and end of retraction (right). The SS rate of each PC is normalized on its mean firing rate from −200 to −100 ms. The rows are sorted according to the maximal modulation during the first 50 ms after the respective movement phase. See also Appendix Figs A3 and A4.

PCs (Proville et al., 2014; Witter et al., 2013). Using an optic fibre with a radius of 200 μm, we increased the SS activity in PCs located within a Euclidian distance of 1 mm (Fig. A1E,F). Whisker movements, most of which were protractions, could be evoked as readily via stimulation in the paramedian lobule and lobule simplex as in crus1 and crus2 (Fig. 1B, C). Yet, different patterns occurred upon stimulation (Fig. 1C–F). For example, optogenetic stimulation of the medial part of the paramedian lobule induced oscillatory movements with different kinematics as compared to those obtained following stimulation of the medial parts of crus1 (Fig. 1D). Stimulation of the medial paramedian lobule for 100 ms evoked whisker movements with a shorter onset latency (108.9 $\pm$ 7.19 ms) compared to medial crus1 (154.4 $\pm$ 4.14 ms; $P = 1.07 \times 10^{-5}$, unpaired t test), (Fig. 1C–E). When we used a shorter period of 50 ms of optogenetic stimulation, the latency (103.63 $\pm$ 5.27 ms) was significantly shorter ($P = 0.02$, paired t test) than that for 100 ms stimulation (132.00 $\pm$ 14.76 ms), highlighting that the evoked whisker movement was linked to the offset, rather than the onset, of the stimulation (Fig. A1). These data are in line with the possibility that a reduction of SS activity at the offset of the stimulation could trigger the whisker movements by disinhibiting and increasing the activity of the CN neurons via a rebound mechanism (Witter et al., 2013). Moreover, the number of whisking cycles made in 1 s after the stimulation was greater for the paramedian lobule (6.36 $\pm$ 1.55) compared to that for crus1 (3.25 $\pm$ 1.31; $P = 9.17 \times 10^{-5}$, unpaired t test), whereas no differences in the maximal change in position or amplitude were observed (i.e. paramedian lobule = 6.78 $\pm$ 0.56° *vs.* crus1 = 6.86 $\pm$ 1.09°; $P = 0.96$, unpaired t test), (Fig. 1F). Instead, stimulation of the medial lobule simplex revealed whisker movements with similar kinematics as those observed upon stimulation of medial crus1 (i.e. maximal amplitude: lobule simplex = 6.20 $\pm$ 1.26° *vs.* crus1 = 6.86 $\pm$ 1.09°; $P = 0.76$, unpaired t-test; latency: lobule simplex = 152.75 $\pm$ 3.90 ms *vs.* crus1 = 154.38 $\pm$ 4.14 ms; $P = 0.84$, unpaired t test; number of cycles: lobule simplex = 3.03 $\pm$ 1.32 *vs.* crus1 = 3.25 $\pm$ 1.31; $P = 0.72$, unpaired t test). Stimulation of the more lateral parts of lobule simplex, the crus1 and crus2 regions, as well as the paramedian lobule resulted in movements with kinematic parameters that were similar to those of medial crus1 (Fig. 1E, F). Thus, optogenetic stimulation of PCs of different medio-lateral parts of the paramedian lobule, crus1 and crus2, and lobule simplex all evoke whisker movements with slightly different

kinematics, but the medial paramedian lobule stands out for its rhythmic movements with relatively short latencies and long durations, highlighting its capability of triggering unique whisker movements.

Purkinje cell activity aligns with whisker movements during spontaneous behaviour

To investigate whether and how SS activity and CS activity encode spontaneous whisker movements, we recorded extracellularly from 233 PCs in different areas of the right cerebellar hemisphere in awake head-fixed mice. We first examined the average whisker position around CSs and SSs to investigate whether spike activity is associated with changes in whisker position (i.e. amplitude) and if such changes preceded or followed the spike activity (Fig. 2A, B). Because each simple spike can in principle be associated with high time-precision whisker changes superimposed on the ongoing oscillation, we aligned whisker position to SS times and found whiskers were significantly more protracted (73/233 cells) or more retracted (62/233 cells) (see Methods for details). Although we did observe a significant change in whisker position also around the CSs (protraction: 73/233 cells, retraction: 34/233 cells), the movement aligned to SSs was larger and earlier for retraction (amplitude of protraction: SS *vs.* CS: 2.68 $\pm$ 0.74° *vs.* 1.17 $\pm$ 0.62°, $P = 1.155 \times 10^{-31}$; amplitude of retraction: SS *vs.* CS: 1.89 $\pm$ 0.84° *vs.* 0.24 $\pm$ 0.16°, $P = 3.79 \times 10^{-22}$; latency of protraction: SS *vs.* CS: 9.5 $\pm$ 24.77 ms *vs.* 12.24 $\pm$ 24.72 ms, $P = 0.3645$; latency of retraction: SS *vs.* CS: 7.06 $\pm$ 24.77 ms *vs.* −7.21 $\pm$ 28.02 ms, $P = 0.005$, paired t test; top and middle panels in Fig. 2C, D). In general, the maximal amplitude of the whisker movements followed rather than preceded SS activity in that maximal protraction and retraction occurred 9.5 $\pm$ 24.77 and 7.06 $\pm$ 24.77 ms after SS activity, respectively. Even though these data indicate that the temporal features of PC activity may allow for a causal bidirectional control of the peak of whisker movements, the onset of the movements frequently preceded the SS times. This finding, which is in line with the correlations observed during other behaviours, such as compensatory eye movements (Voges et al., 2017), suggests that SS activity could play a role in coordinating initiation and modulation of whisker movements.

To visualize how PCs associated with protraction or retraction are spatially distributed across the recorded areas, we plotted the mean whisker modulation in a 100 ms period around SS or CS activity in the approximate
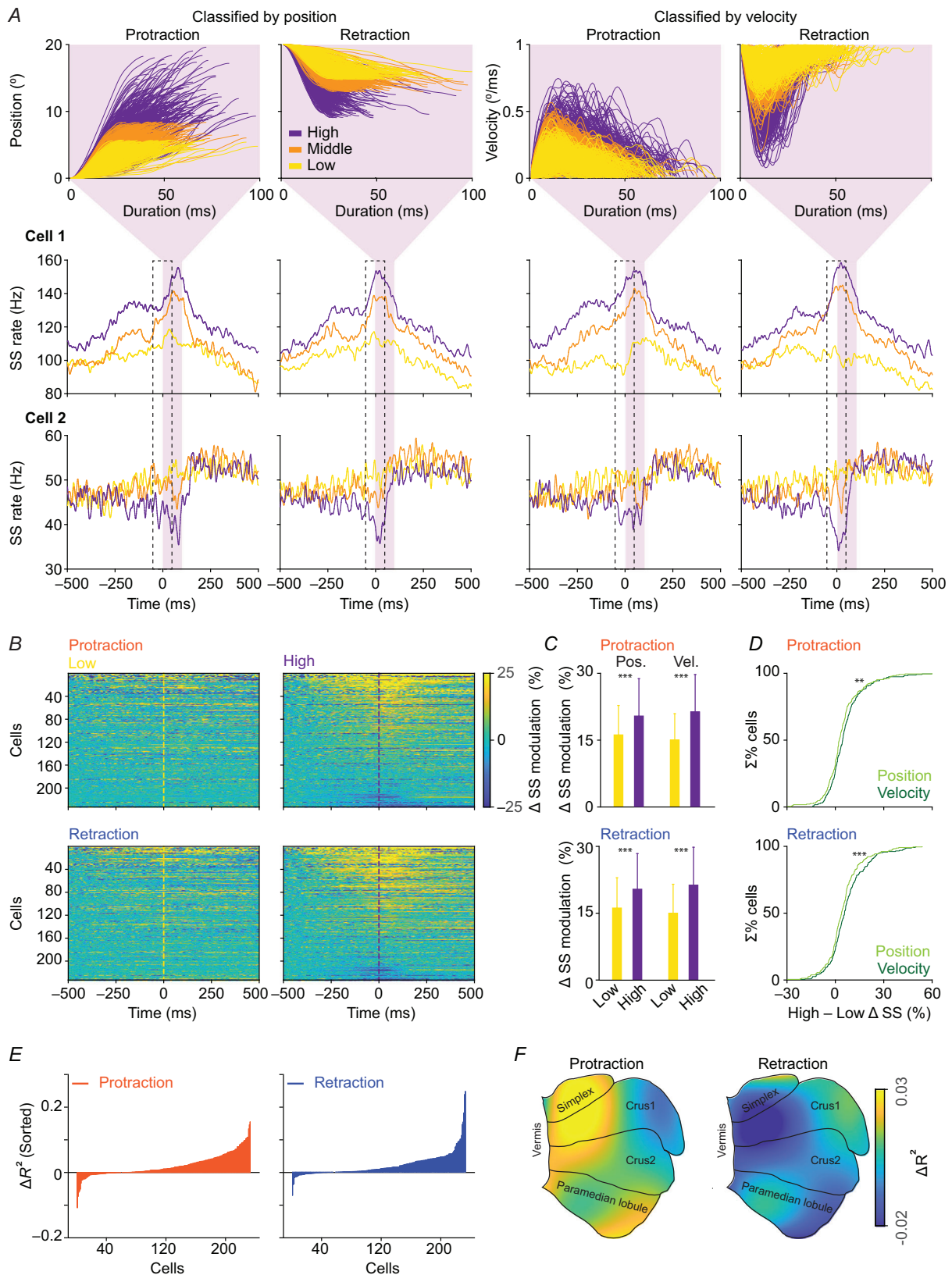
Figure 4. Purkinje cells encode not only the position but also velocity of whiskers
A, based on the level of position (left two columns) or velocity (right two columns), each protraction and retraction was classified into one of three groups (low, middle and high indicated in yellow, orange and purple, respectively). To assess the sensitivity of the simple spike (SS) activity of each PC for the position or velocity of protractions and

retractions we calculated and plotted the average SS rate during the initial 100 ms window of the movements with the low, middle and high levels of position and velocity (highlighted by the dashed boxes). The cells showed heterogeneous responses with either an increase (i.e. SS facilitation) or a decrease of their SS firing rate (i.e. SS suppression). The magnitude of both SS facilitations (Cell 1, middle row) and SS suppressions (Cell 2, lower row) scaled well with the low, middle and high groups. In general, the sensitivity for the velocity of both protractions and retractions appeared relatively stronger compared to position. For example, Cell 1 (middle row) and Cell 2 (lower row) show greater differences between their SS firing rate associated with high and low levels of velocity (distance between the yellow and the purple line, right), compared to high and low levels of position (left). Note that the shaded areas in purple indicate the time period used for grouping whisking movements, while the dashed boxes indicate the time window used for PC activity analysis (from −50 to 50 ms after the start of the retraction or protraction). *B*, the SS modulation of the entire population of the 233 PCs is shown as a heatmap where each row represents one cell. The cells are sorted according to the maximal modulation in the 150 ms after the start of protraction (top row) and retraction (bottom row). The heatmaps are shown for movements with low (left) and high (right) levels of velocity. Dashed lines indicate the start of the whisker movement. *C*, bar plots indicating that the changes in SS rate (from −50 to 50 ms after the start of the protraction or retraction) for the group high (purple) was bigger than for the group low (yellow) both when sorting according to the position change or velocity (high *vs.* low for protraction $P = 5.11 \times 10^{-8}$ for position and $P = 2.32 \times 10^{-15}$ for velocity; high *vs.* low for retraction $P = 3.08 \times 10^{-10}$ for position and $P = 1.10 \times 10^{-17}$ for velocity, paired *t* test). *D*, however, the difference between the two groups was smaller when sorting by amplitude compared to velocity ($P = 0.004$ for protraction and $P = 0.0002$ for retraction, paired *t* test), indicating higher SS sensitivity for the latter. The preference for velocity sensitivity was confirmed by comparing the linear fitting of the correlation between each individual segment of whisker movement (i.e. protraction and retraction) and the corresponding SS rate (*D*). Bar plots with sorted differences in R^2 (difference between the R^2 obtained correlating position or velocity with SS rate) for individual cells from −50 to 50 ms after the start of the protraction (left) or retraction (right). These plots show that the firing rate of most cells correlates better with velocity (positive values) than with position (negative values). At the population level, the R^2 for velocity was significantly higher than that for position during both protraction and retraction (for protraction $P = 6.29 \times 10^{-4}$; for retraction $P = 8.45 \times 10^{-4}$; Wilcoxon paired test). *F*, the spatial plot of the differences in R^2 values between velocity and position sensitivity of each cell in the approximate location where it is recorded. The lobule simplex, medial crus1 and crus2 as well as the lateral paramedian lobule contain many PCs with a prevalent SS sensitivity for velocity during protraction, while velocity during retraction is mainly encoded in the lateral crus1 and medial paramedian. Error bars in *C* indicate the standard deviation. See also Appendix Figs A5–A8.

location where each PC was recorded from (bottom panels in Fig. 2*C*, *D*). PCs with SS activity associated with protraction and retraction were particularly abundant in lateral crus1 and lateral paramedian lobule, respectively. Instead, the PCs with CS activity associated with protraction and retraction showed the opposite distribution pattern (Fig. 2*C*, *D*; for more details, see Fig. A2). For example, PCs with CS modulations associated with protraction were particularly abundant in the lateral paramedian lobule pattern (Fig. 2*D* bottom right).

Simple spikes encode different phases of the whisker movements

Previously, it has been reported that PCs of crus1 encode the slow component of whisker position (i.e. whisker midpoint), but not the fast component associated with the phase of the whisking cycle (Chen et al., 2016). We performed a phase transformation and also found weak correlations between SS activity and phase of the whisking cycle for PCs of lobules other than crus1 (Fig. A3). Based on the quasiperiodic element of whisking and that PCs could signal timing rather than the whisking phase, we analysed the fast component of whisking behaviour for individual whisk segments (Towal & Hartmann, 2008;

Wineski, 1983). We filtered out the slow component (< 2 Hz) to align the whisker baseline to 0 and examined PC activity at the beginning and end of each individual protraction or retraction (Fig. 3, Fig. A4*B*, for details see Methods). The end of a whisk in one direction frequently corresponded in time to the start of the subsequent whisk in the opposite direction, but occasionally two consecutive whisker movements were separated by a transient delay (Fig. 3*A*). When we examined SS activity around the four time-points of interest, that is start of protraction, end of protraction, start of retraction, and end of retraction, the SS modulation around the time-points of interest differed greatly across PCs (see, for example, in Fig. 3*B* cells 1−6). Whereas some cells showed unidirectional modulation that could be either an increase (cell 2) or a decrease (cell 3) of SS activity, other cells showed more complex patterns of bidirectional modulation (cells 5 and 6). When aligning the SS modulation of all 233 recorded cells to the time-point of interest (Fig. 3*C*), we observed that the most prominent changes in SS activity concerned increases shortly after the beginning of a protraction [maximal modulation after (0 to 50 ms) – before (−50 to 0 ms): start of protraction $= 1.73 \pm 0.28\%$, end of protraction $= 0.06 \pm 0.27\%$, start of retraction $= -0.27 \pm 0.36\%$, end of retraction $= -1.19 \pm 0.38\%$]. The modulation after
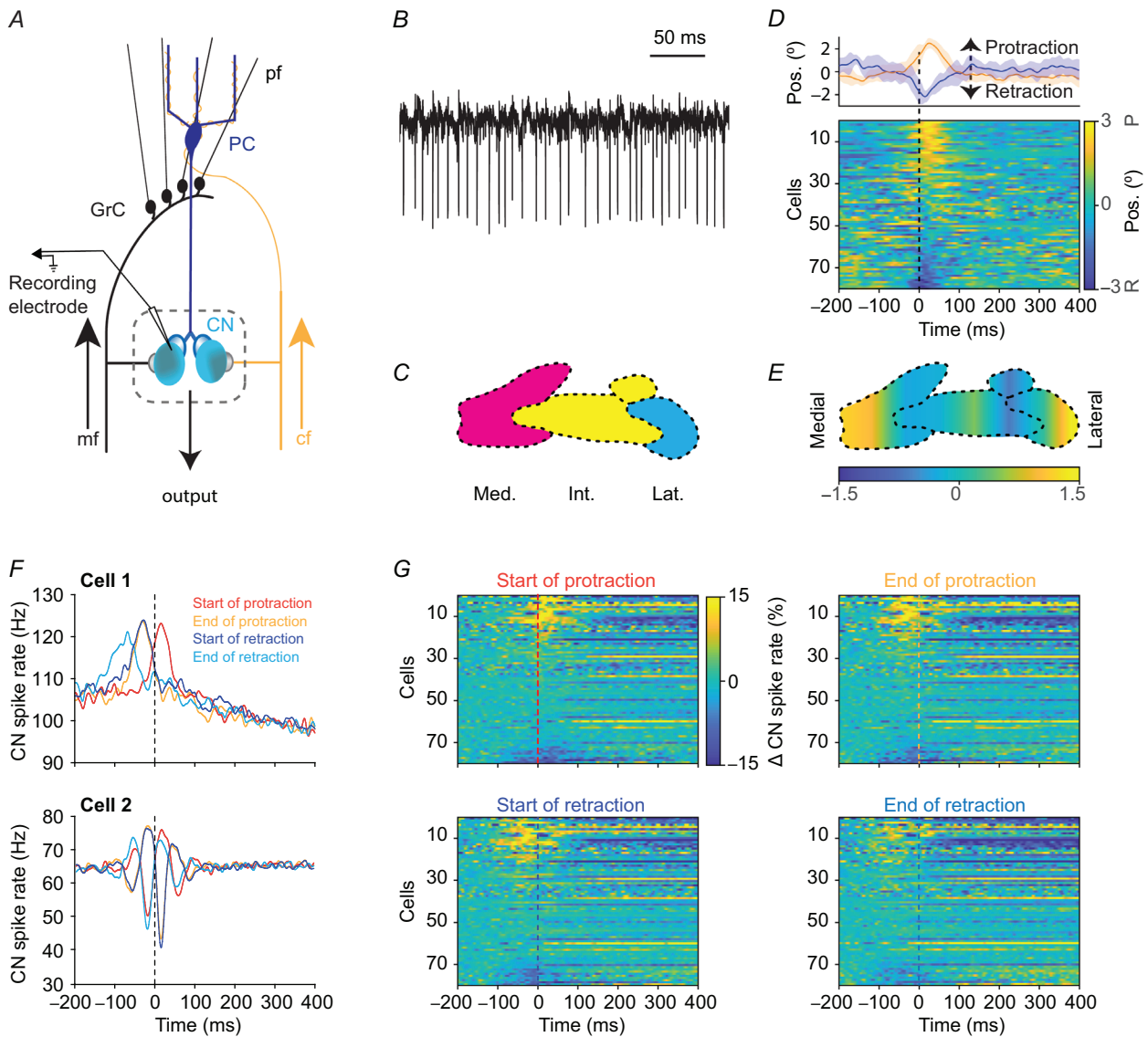
Figure 5. Spikes of cerebellar nuclei neurons encode the different phases of the whisker protractions or retractions with heterogeneous firing patterns

A, the cerebellar cortex receives inputs from the climbing fibres (cfs) and mossy fibres (mf), the latter of which activate the granule cells (GrC) giving rise to the parallel fibres (pfs). The signals from these inputs are relayed via the Purkinje cells (PCs) to the cerebellar nuclei (CN) where ultimately all information is integrated with cf and mf collaterals and recorded. *B*, an example of a raw recording of the activity of a CN neuron. *C*, a schematic of the three CN; the blue, yellow and pink structures indicate the lateral (Lat), interposed (Int) and medial (Med) CN. *D*, whisker movements around CN neuron firing are represented in a heatmap with each row representing the average whisker position for each recorded CN neuron; positive values (yellow) represent protraction (P) and negative values represent retraction (R). The rows are sorted according to the mean whisker position (during the first 50 ms after the onset of spike time). The neurons for which the spike activity preceded whisker protraction (top part of the heatmap in yellow) can be distinguished from cells for which the activity preceded whisker retraction (bottom part of the heatmap in blue). The average whisker position for these two groups of cells is shown above the heatmap. The orange and blue lines represent the average whisker modulation for the cells (12 out of 78 for each group) that exceeded one SD above or below the mean, respectively. The shaded areas around the lines represent the standard deviation. *E*, schematic of the spatial distribution of recorded CN neurons in the mediolateral plane. The colours represent the mean whisker movement during the first 50 ms after CN neuron firing. The CN neurons associated with protraction were preferably located either very medial (medial portion of the medial CN) or very lateral (lateral part of the lateral CN). *F*, convolved peri-event time histogram (PETH) of two different examples of CN neurons with different preferences for the different phases. The dark and light orange and the dark and light blue represent the CN neuron modulation around the time of the start of protraction, end of protraction, start of retraction and end of retraction, respectively. *G*, spike activity of all 78 recorded CN neurons is shown as a heatmap raster plot and aligned to the start of protraction (top left), the end of protraction (top right), the start of retraction

(bottom left) and the end of retraction (bottom right). The spike rate of each CN neuron is normalized based on the mean of its firing rate from −200 to −100 ms. The lines are sorted according to the maximal modulation during the first 50 ms after the start of protraction. See also Appendix Fig. A9.

the beginning of a protraction was significantly bigger than the second most prominent modulation (i.e. end of retraction; |start of protraction| *vs.* |end of retraction|, $P = 0.037$, paired *t* test). This differential modulation around the time-point of interest indicates that the PC SS activity also encodes the fast component of whisking. Albeit less prominent, heterogeneous patterns of activity were also observed for CSs [maximal modulation after (0 to 50 ms) – before (−50 to 0 ms): start of protraction = 0.03 ± 0.08%, end of protraction = −0.18 ± 0.05%, start of retraction = −1.3 ± 0.06%, end of retraction = −0.25 ± 0.06%; |start of protraction SS| *vs.* |start of protraction CS|, $P = 1.13 \times 10^{-9}$, paired *t* test] (Fig. A4*C,D*). We conclude that, in addition to the setpoint (Chen et al., 2016), PC activity also encodes the fast component of whisking.

Purkinje cells encode not only the position but also the velocity of whiskers

Based on the heterogeneity of SS modulation across the PC population, we hypothesized that SS activity of different PCs could be tuned to different whisker kinematic parameters. SS modulation in crus1 PCs has been found to linearly encode whisker position, in particular that of the midpoint (Chen et al., 2016), whereas SS modulation in PCs of other regions such as the flocculus of the vestibulocerebellum or the oculomotor vermis is predominantly tuned to the velocity of eye movements (Herzfeld et al., 2015; Sedaghat-Nejad et al., 2022). To determine to what extent PCs of the different lobules in the cerebellar hemispheres encode different whisker kinematic parameters (i.e. position and/or velocity), we examined the SS activity of individual PCs on their sensitivities for position change (i.e. amplitude of the segment of a whisk from the starting point to the end point; see scheme in Fig. A4*B*) and velocity of protraction and retraction movements. For each of the four categories (i.e. position during protraction, position during retraction, velocity during protraction and velocity during retraction), we divided the individual whisker movements evenly into three groups with different levels of velocity or position change (0–33.3% referred to as low; 33.3–66.6% as middle; or >66.6% as high; Fig. 4*A*). When we quantified the change of SS rate during the 100 ms window around the onset of protractions and retractions, we observed that the SS modulation was maximal for the 'high' group independent of whether we

sorted by position change (i.e. amplitude) or by velocity (percentage of modulation from baseline SS firing for protraction amplitude: high: 22.69 ± 17.46%, middle: 20.17 ± 16.07%, low: 18.04 ± 13.84%; modulation for retraction amplitude: high: 23.09 ± 17.22%, middle: 20.03 ± 15.19%, low: 18.04 ± 14.88%; modulation for protraction velocity: high: 22.91 ± 17.10%, middle: 20.40 ± 15.33%, low: 17.13 ± 13.17%; modulation for retraction velocity: high: 24.67 ± 18.90%, middle: 19.66 ± 14.8%, low: 17.59 ± 14.47%; Fig. 4*B,C*).

To better assess the sensitivity of the SS activity of each PC for the position or velocity of protractions and retractions, we calculated the difference between the 'high' and 'low' groups in SS modulation following grouping based on velocity or position (Fig. 4*D*). Even though the PCs ($n = 233$) showed heterogeneous responses, the sensitivities for the velocity during protractions and retractions were higher than those for position ($P = 0.004$ for protraction and $P = 0.0002$ for retraction, paired *t* test). This preference for velocity sensitivity was confirmed also when, instead of grouping, the instantaneous SS rate was correlated with either amplitude or velocity of each individual whisking segment (Fig. 4*E*; Fig. A8*C*). Moreover, at the population level, the R^2 value for velocity was also significantly higher than that for position during both protraction and retraction (for protraction $P = 6.29 \times 10^{-4}$; for retraction $P = 8.45 \times 10^{-4}$, Wilcoxon paired test). The PCs with a prevalent SS sensitivity for velocity during protraction were predominantly located in the lobule simplex, medial crus1 and crus2 as well as in the lateral paramedian lobule. The PCs with a prominent velocity sensitivity during retraction were mainly situated in the lateral paramedian and lateral crus1 (Fig. 4*F*; for details see also Fig. A5).

To test whether the PCs exhibiting high correlations with the fast-whisking component are the same as exhibiting strong correlation with the slow-whisking component we also calculated the correlations between SS activity and the amplitude (Fig. A6) and midpoint (Fig. A7) of the whisking envelope. The PCs that correlated well with the slow whisking component differed from those correlating with the fast component (Fig. A8*A, B*). Instead, the PCs with strong correlations with the amplitude of the fast component were the same as those with strong correlations with the velocity of the fast component. The fact that the SS correlation with velocity was generally stronger than that with the amplitude also emerged from the latter analysis, as the data points of this correlation were mostly located above the diagonal in the plot (Fig. A8*C, D*).
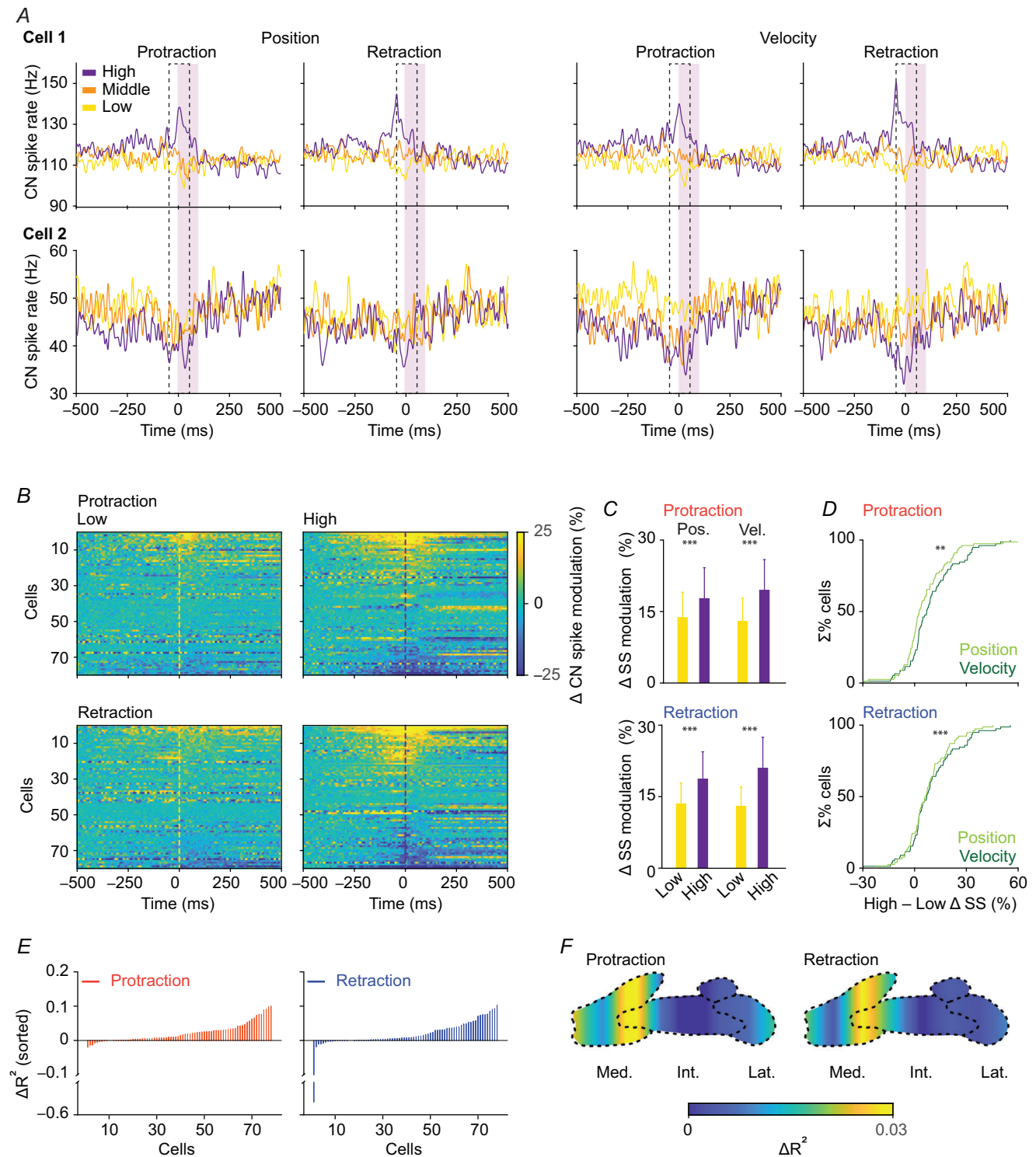
Figure 6. The cerebellar nuclei neurons also encode both whisker position and velocity
A, the convolved peri-event time histograms (PETH) of two examples of CN neurons: one that increases (Cell 1, top row) and another one that decreases (Cell 2, bottom row) its firing rate around protraction (left and middle-right) and retraction (middle-left and right). Note that for these two different cells the maximal modulation was obtained when aligning the activity for retraction and relating it to velocity (rightmost column). The shaded area indicates the time period used for grouping whisking movements, and the dashed frame indicates the time window we used for CN neuron activity analysis. *B*, the spike modulation of the entire population (*n* = 78 cells) is shown as a heatmap where each row represents one cell. The cells are sorted according to the maximal modulation in the 150 ms after the start of protractions (top row) and retractions (bottom row) occurring at low (left) and high

(right) levels of velocity. Dashed lines indicate the start of the whisker movement. *C*, bar plots indicating that the change in CN spike rate (from −50 to 50 ms after the start of the protraction or retraction) for the group high (purple) was greater than for the group low (yellow) both when sorting according to the position and the velocity (high *vs.* low for protraction $P = 5.72 \times 10^{-4}$ for position and $P = 1.7 \times 10^{-7}$ for velocity; high *vs.* low for retraction $P = 3.54 \times 10^{-7}$ for position and $P = 9.71 \times 10^{-11}$ for velocity, paired *t* test). *D*, similarly to PC, also for CN neurons, the difference between the two groups was smaller sorting by amplitude compared to velocity ($P = 0.001$ for protraction and $P = 0.004$ for retraction, paired *t* test), indicating higher SS sensitivity for the latter. The preference for velocity sensitivity was confirmed by comparing the linear correlation between each individual segment of whisker movement (i.e. protraction and retraction) and the corresponding CN spike rate (*D*). *E*, sorted differences in R^2 (difference between position and velocity sensitivity) for individual CN neurons from −50 to 50 ms after the start of the protraction (left) or retraction (right). The bar plots of differences in CN modulation show that the firing rate of most cells correlates better with velocity (positive values) than with position (negative values). Likewise, at the population level, the R^2 for velocity was higher than that for position during both protraction and retraction (for protraction $P = 0.0019$, for retraction: $P = 0.0207$; Wilcoxon paired test). *F*, plot of the difference of R^2 values for each cell in the approximate location where CN neurons were recorded. The portions of CN that modulate more for velocity (medial part of CN; highest values indicated in yellow) is similar for protractions (left) and retractions (right). See also Appendix Fig. A10.

Cerebellar nuclei neurons encode different phases of whisker movements

PC activity is conveyed to premotor neurons via CN neurons. To investigate whether CN neurons preferentially modulate their activity with protraction or retraction, we calculated the average whisker position around the time of each spike of 78 CN neurons (Fig. 5*A*, *B*; see also Methods for details). As with SS activity in PCs, the spikes of CN neurons preceded predominantly whisker protraction, but even so, a substantial amount preceded retractions (cell number: protraction *vs.* retraction: 32/78 *vs.* 17/78; amplitude: protraction *vs.* retraction: 2.53 ± 0.58° *vs.* 2.43 ± 0.73°; latency: protraction *vs.* retraction: 25.50 ± 23.64 ms *vs.* 8.24 ± 28.39 ms) (Fig. 5*C*, *D*). Based on the mediolateral position of insertion of the recording electrode, it was possible to retrieve the approximate mediolateral location of each CN neuron (Fig. 5*E*; see Methods). The CN neurons that were preferentially related to protraction were located in the medial and lateral CN, whereas the interposed nuclei showed a mixed prevalence for protractions and retractions (Fig. 5*E*; for details see also Fig. A9). Next, we aligned CN neuron spiking with the four time-points of interest determining the start and the end of protraction and retraction (Fig. 5*F*, *G*). As with PCs, some CN neurons exhibited unidirectional modulation (i.e. a transient increase or decrease of their firing rate; Fig. 5*F* top panel), whereas others showed more complex patterns of modulation (e.g. a succession of increase and decrease of firing rate; Fig. 5*F* bottom panel). The activity of CN neurons increased after the start and the end of the protraction [maximal modulation after (0 to 50 ms) – before (−50 to 0 ms): start of protraction = 0.73 ± 0.25%, end of protraction = 0.34 ± 0.34%] and decreased during and after the end of retraction [maximal modulation after (0 to 50 ms) – before (−50 to 0 ms): start of retraction = −0.13 ± 0.31%, end of

retraction = −1.17 ± 0.34%, $P = 0.05$, paired *t* test; Fig. 5*G*].

Cerebellar nuclei neurons also encode both whisker position and velocity

CN neurons ($n = 78$) were, similar to the PCs, preferentially tuned to whisker velocity or whisker position. As done for the analysis of PC modulation, we grouped the individual whisker movements as either low, medium or high according to the velocity level or position change, and we subsequently assessed to which of the two kinematic parameters each CN neuron was preferentially tuned (Fig. 6*A*). In line with their convolved peri-event time histograms (PETHs) we found that the majority of CN neurons preferentially modulated with velocity rather than with position change (Fig. 6*B*, *C*). These findings were observed for both protraction and retraction. The sorted differences in R^2 (difference between position and velocity sensitivity) for individual cells from −50 to +50 ms around the start of the protraction or retraction also highlighted their preference for velocity signals (Fig. 6*D*). Indeed, at the population level, the R^2 for velocity was significantly higher than that for position during both protraction and retraction (for protraction: $P = 0.0019$, for retraction: $P = 0.02$; Wilcoxon paired test). Interestingly, in terms of localization the CN regions that contained most cells sensitive to velocity of protraction coincided with those of the CN cells sensitive to velocity of retraction, that is the medial and interposed CN (Fig. 6*D*; for details see also Fig. A10). Thus, despite the firing patterns being heterogeneous across the neuronal population, there is a region-specific modulation of CN neuron activity that encodes the two phases (i.e. protraction and retraction) of the fast component of whisker movements with a clear adherence to velocity encoding.

Discussion

Sensory orofacial representation studies by Welker and colleagues revealed more than 40 years ago that natural stimulation of different parts of the whisker pad can result in short-latency, large-amplitude responses in multiple patches of the cerebellar cortex (Shambes et al., 1978). Yet, to what extent these parts of the cerebellum may control motor activity of the corresponding facial regions has remained relatively poorly understood. In this study, we performed region-specific optogenetic stimulation of PCs in four different lobules of the cerebellar hemispheres to investigate their potential role in controlling the kinematics of whisker movements and we explored whether the activity of these PCs as well as that of their CN target neurons encode different kinematic parameters during spontaneous whisker movements. Both the stimulation and recording experiments highlight that not only PC–CN microcomplexes comprising crus1 and crus2, but also those comprising the paramedian lobule and lobule simplex may contribute to kinematic control of whisker movements, in particular that of their velocity.

Motor control by the paramedian lobule and lobule simplex

Our data show that stimulation of PCs in the paramedian lobule is particularly effective in generating short-latency, long-lasting rhythmic whisker movements. Thus, even though the whisker receptive fields in the paramedian lobule may be smaller than those in crus1 and crus2 (Shambes et al., 1978), this does not directly imply that they have a lesser role in motor coordination; in fact, it might even mean the opposite in that they might take advantage of the smaller fields and thereby exert fine-tuning control at a higher spatial resolution. Along the same vein, one might speculate that the crus regions are more specialized in receiving and processing sensory information (Bosman et al., 2010; Shambes et al., 1978), whereas the paramedian lobule might be more strongly implicated in motor control. Given that the paramedian lobule, crus regions and also lobule simplex are all participating in the same microcomplexes and olivocerebellar micromodules (Beekhof et al., 2021; De Zeeuw, 2021), sensorimotor integration could be facilitated by the recurrent loops of these networks (Apps & Hawkes, 2009; Chaumont et al., 2013; De Zeeuw et al., 2011; Miall et al., 1998) and even play a role in controlling the rhythmicity of the whisker movements (Bauer et al., 2022; Lang et al., 2006). Another possibility, which is not mutually exclusive with the former suggestion, is that PCs in different cerebellar lobules compute different aspects of sensory and motor processing, such as differential dynamics with faster and slower components that may depend on lobule-specific mossy fibre inputs (Chen et al., 2016).

Involvement of the paramedian lobule in motor control has previously also been shown for limb movements. Stimulation of forelimb-related neocortical regions in rat induces c-fos expression in the paramedian lobule (Sharp et al., 1989); SS activity of PCs in the paramedian lobule can be time-locked to the step cycle of awake cats on a treadmill (Apps & Lidierth, 1989); and local field potential oscillations are most prominent in the paramedian lobule of primates during voluntary limb movements (Pellerin & Lamarre, 1997). Therefore, one might hypothesize that the paramedian lobule is involved in active exploration of the environment, be it with the limbs and/or with the whiskers.

The lobule simplex has also been considered previously in coordination of movements, in particular that of eye and eyelid movements. For example, PC activity in the lobule simplex of rhesus monkeys correlates strongly with the velocity of horizontal eye movements (Marple-Horvat & Stein, 1990). Likewise, PCs in the lobule simplex of mice play a role in delay eyeblink conditioning (Heiney, Wohl et al., 2014; ten Brinke et al., 2015; Wang et al., 2020), while those in rabbits have been shown to contribute to conditioning of the nictitating membrane response (Schreurs et al., 1991). The current findings on a potential role of PCs in the murine lobule simplex in controlling kinematics of whisker movements are in line with the observations by Sharp & Gonzalez (1985), who showed that stimulation of the whiskers in rats alters activity in the lobule simplex. Hence, the lobule simplex may also play a role in active exploration of the environment, but different from that of the paramedian lobule, with the use of whisker and eye movements rather than whisker and limb movements. Interestingly, both the lobule simplex and paramedian lobule converge in part on the interposed nucleus, which has recently been shown to integrate control of limbs and facial musculature, during a more general defensive response (Heiney et al., 2021).

Simple spike and complex spike activity during whisker movements

The SS and CS activity of the PCs investigated here for four lobules in the right cerebellar hemisphere probably serve different roles in sensorimotor integration during spontaneous whisker movements. SSs scaled well with specific kinematics of the whisker movements, in particular their velocity. Similar correlations have been found for other behaviours, including compensatory eye movements (De Zeeuw et al., 1995), saccadic eye movements (Herzfeld et al., 2015) and limb movements (Hewitt et al., 2011).

Because optogenetic manipulation of SS activity has been shown to affect both the amplitude and speed of movements (Heiney, Kim et al., 2014; Proville et al., 2014; Witter et al., 2013), it was unclear whether SS activity of different clusters of PCs may preferentially encode the amplitude or the velocity of the movement. For the whisker system, it has already been shown that SS activity of PCs of crus1 encodes the position and predicts the whisker setpoint (Chen et al., 2016). Here, we also find evidence that SSs of some PCs encode the slow component of the whisker movement (Chen et al., 2016) (Figs A6 and A7). In addition, we found that SSs of relatively many PCs encode both the position and velocity of the fast component of whisker movement. Interestingly, we found that, while a minority of PCs correlated better with whisker position, the majority correlated best with velocity of the fast components (Fig. 4*C*, *D*). This result is in line with studies on other motor behaviours for which position, direction and velocity are widely and robustly encoded in the activity of cerebellar neurons (Ebner et al., 2011). The fact that each PC exhibits different tuning sensitivity for fast and slow whisking components (Fig. 8*A*, *B*) suggests that the cerebellum processes movements taking place at multiple time scales by distributing different kinematic parameters across different groups of PCs. Analysis of the anatomical distribution of PCs correlating with velocity revealed clear alternating patterns of activity for protraction and retraction (Fig. 4*E*). The fact that we did not detect a clear spatial segregation between PCs encoding velocity and amplitude of the movement suggests that PCs encoding different kinematic parameters may be intermingled within the same upbound or downbound microzone (De Zeeuw, 2021).

This is different for CSs, which adhere to the microzones and micromodules by definition (De Zeeuw, 2021). CSs can be associated with the initiation or interruption of voluntary limb movements (De Gruijl et al., 2014; Hoogland et al., 2015), with sequences of tongue or whisker movements, sometimes even in bilateral synchronous patterns (Romano et al., 2022), and/or reward-based acquired tasks (Bina et al., 2021; Heffley & Hull, 2019; Kostadinov et al., 2019; Wagner et al., 2021). Here, we showed that the encodings of CS activity of PCs for protractions and retractions of the whiskers in the paramedian and simplex lobules as well as the crus regions were distributed in a pattern opposite to that for the preferred encodings of the SS modulations. Moreover, the kinematics of the whisker movements were less prominently represented in the CS activity than in the SS activity, and the latency of the CS activity showed less heterogeneous patterns with respect to the start and end of the whisker movements. Together, our data suggest that the CS activity may be more likely to determine the state of a particular sensory saliency or state of behaviour (Bina

et al., 2021), while SS activity may be more prominently involved in controlling the precise kinematics of the related motor performance.

Cerebellar nuclei neurons encode either velocity or amplitude during voluntary whisking

The PCs, which form the sole output of the cerebellar cortex, converge on the downstream vestibular and CN neurons (Person & Raman, 2012), which in turn represent the sole output of the entire cerebellum. CN neuron spike activity can affect motor behaviour in health and disease (White & Sillitoe, 2017). However, the way in which CN neuron spike activity is modulated during self-generated movement can be complex (Brooks et al., 2015). We found that CN neuron spike activity also encodes precise kinematics of whisker movement, similar to PCs (Figs 5 and 6). The presence of CN neurons with modulation preferably tuned to amplitude or velocity of the movements and with complementary activity during protraction and retraction suggests that PC whisker-related inputs are reliably conveyed by CN neurons to the downstream premotor neurons controlling whisker movements (Hattox et al., 2002; Teune et al., 2000). Interestingly, during retraction, we found that CN neurons that modulated predominately with velocity were located medially (Fig. 6*D*). This raises the possibility that different cerebellar nuclei could control specific movement kinematics. Future studies, in which the PC activity and CN neuron activity of specific upbound and downbound microcomplexes are studied with respect to specific kinematic parameters, including those of the whisker movements, could reveal the functional relevance of cerebellar modules (De Zeeuw, 2021).

Zonal distribution of Purkinje cells and cerebellar nuclei neurons encoding voluntary whisking

PCs provide tonic inhibition to CN neurons of the longitudinal zone to which they belong (Apps et al., 2018; Person & Raman, 2011; Sugihara et al., 2009). It follows that for the zones in which the SS activity was positively correlated with protraction, CN neuron activity is expected to be negatively associated with movements in this direction (De Zeeuw, 2021). Indeed, while in the cerebellar cortex the PCs with SS modulation associated with protraction were predominantly located laterally (bottom panels in Fig. 2*C*, *D*), the CN neurons associated with protraction were predominantly located medially (Fig. 5*E*). A few CN neurons correlating with protraction, however, were also present in the most lateral part of the CN. These CN neurons exhibited complementary activity patterns to the PCs associated with retraction located in the lateral paramedian. Interestingly, these PCs

have CS activity associated with protraction. Therefore, in these PCs with SSs associated with retraction, the CS-induced SS pause could correspond to spiking activity in the most lateral part of the CN and induce whisker protraction. This possibility is in line with the finding that SS and CS activity in the oculomotor vermis is associated with saccade movements in opposite directions (Sedaghat-Nejad et al., 2022). These converging results raise the intriguing possibility that, in some PCs, CSs and SSs could be responsible for bidirectional motor control, yet in opposite directions.

Conclusion

This study focused on mapping the whisker motor representations on a large part of the cerebellar cortex.

We found that the medial part of the paramedian lobule, an area that was known to have only a relatively small whisker sensory receptive field, is one of the key areas to induce rhythmic whisker movement, and that the lobule simplex may exert similar functions as the crus regions. We found distinct areas with complementary activity for alternating movement in opposite directions (i.e. protraction and retraction). The prevalence of SS modulation for whisker velocity or amplitude was complementary during retraction and protraction. Finally, we revealed a medio-lateral organization for CN neurons, the spike activity of which is complementary to that of SSs of PCs.
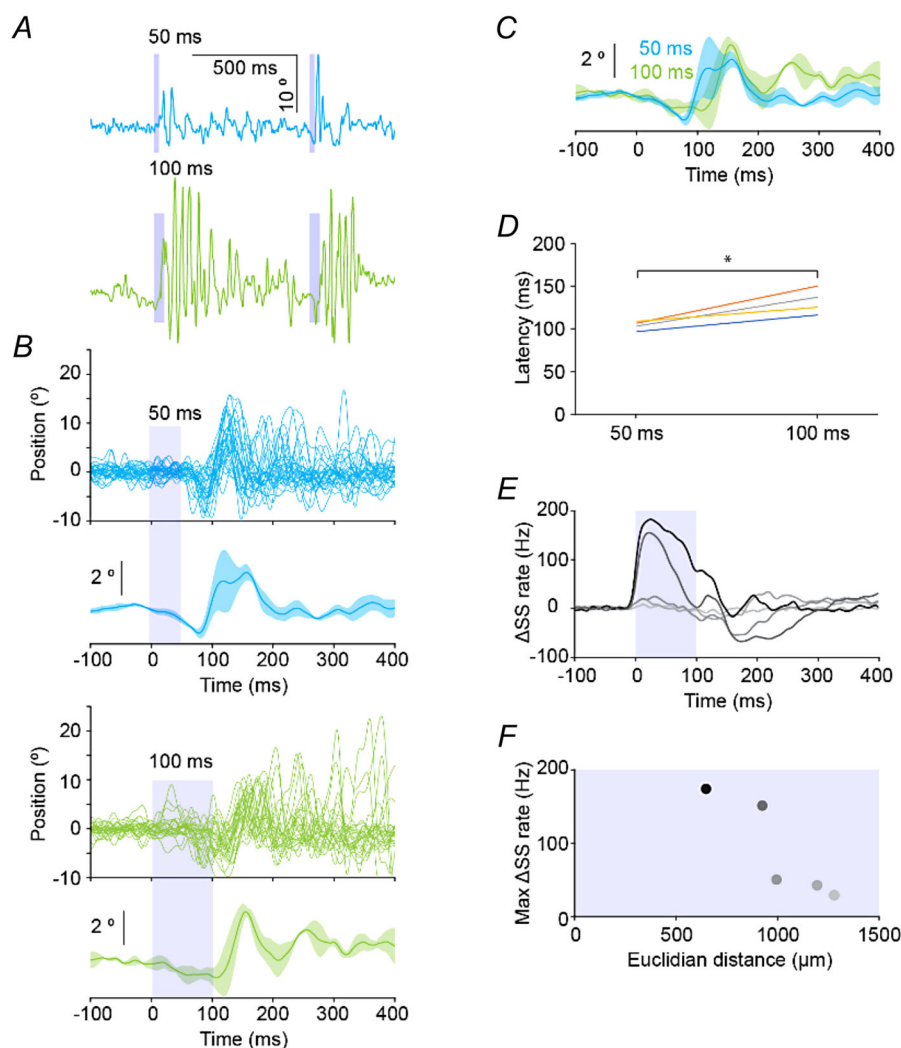
Appendix

Figure A1.

Different durations of optogenetic stimulation of PCs induce whisker movements with different onset latency. *A*, two consecutive optogenetic stimulations of PCs in the medial paramedian lobule, with a duration of either 50 ms (top) or 100 ms (bottom). *B*, examples of whisker movements of individual trials following 50 ms (top) or 100 ms (bottom) optogenetic stimulation, as well as the average whisker movements of four mice following such stimulation. *C*, the whisker movements induced using the two different stimulus durations are overlapped for comparison. *D*, onset latency of the whisker movement following 50 ms optogenetic stimulation is significantly shorter than that for 100 ms stimulation (when calculated from the onset of the stimulus), highlighting the impact of the different stimulus offset. Each line indicates one mouse. Asterisks indicate $P = 0.02$. *E*, SS spike modulation of five Purkinje cells recorded during optogenetic stimulation. Each Purkinje cell was recorded at a different Euclidian distance from the stimulation fibre. *F*, plotting the maximal change in SS rate as a function of Euclidian distance, we estimated that, under our experimental conditions, we mostly activated PCs located within 1000 μm from the fibre (see also Methods for details).
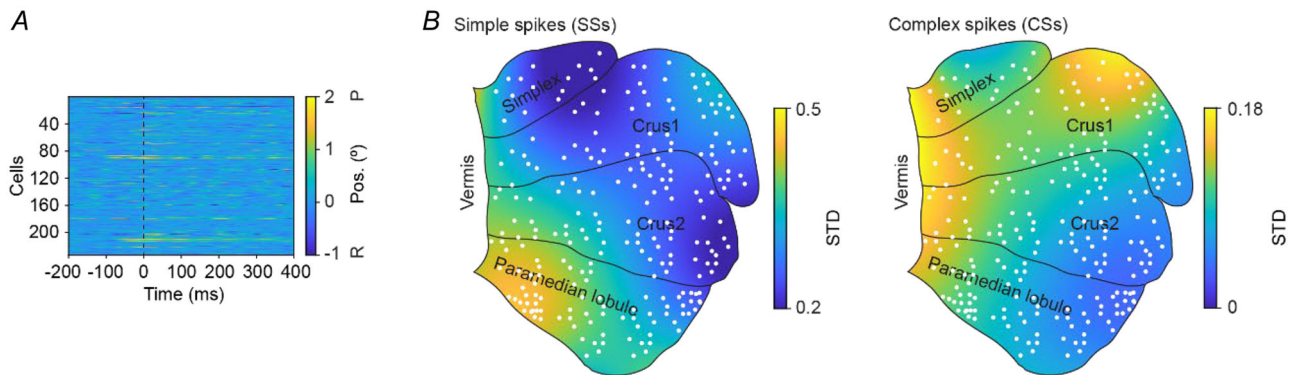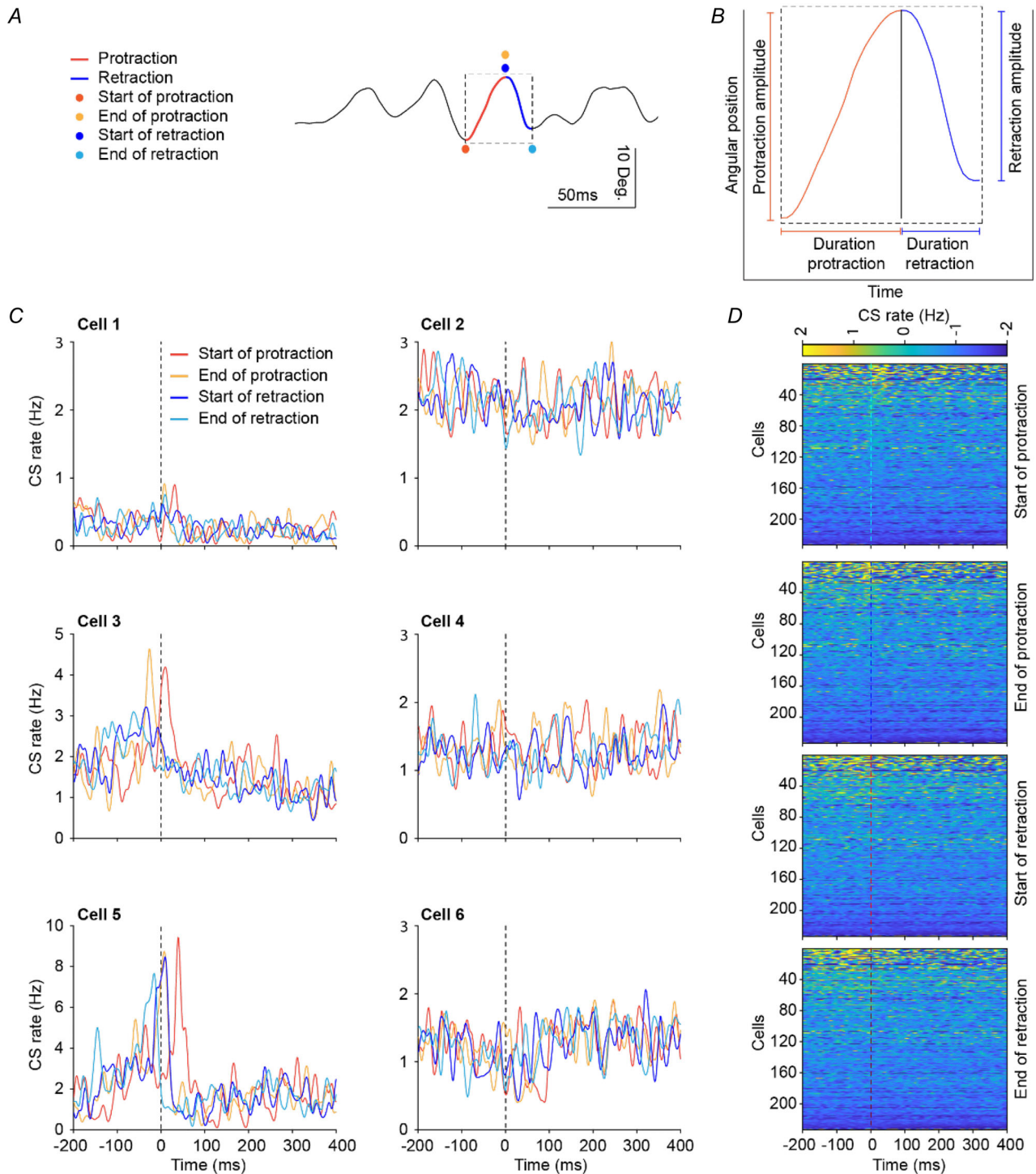

Figure A2.
A, whisker modulation around the CSs plotted according to the order of magnitude of the modulations of SSs (i.e. same order as in Fig. 2*C*). Instead, the data of the heatmap of Fig. 2*D* are plotted according to the order of the CS mean whisker position during the first 50 ms after the CS. *B*, the variability relative to the heatmap of Fig. 2*C* and *D* is shown for each region of the cerebellar hemisphere. The colour code indicates the standard deviation of the change in whisker position associated with SS (top) or CS (bottom). Each white dot represents the approximate location where each PC was recorded.
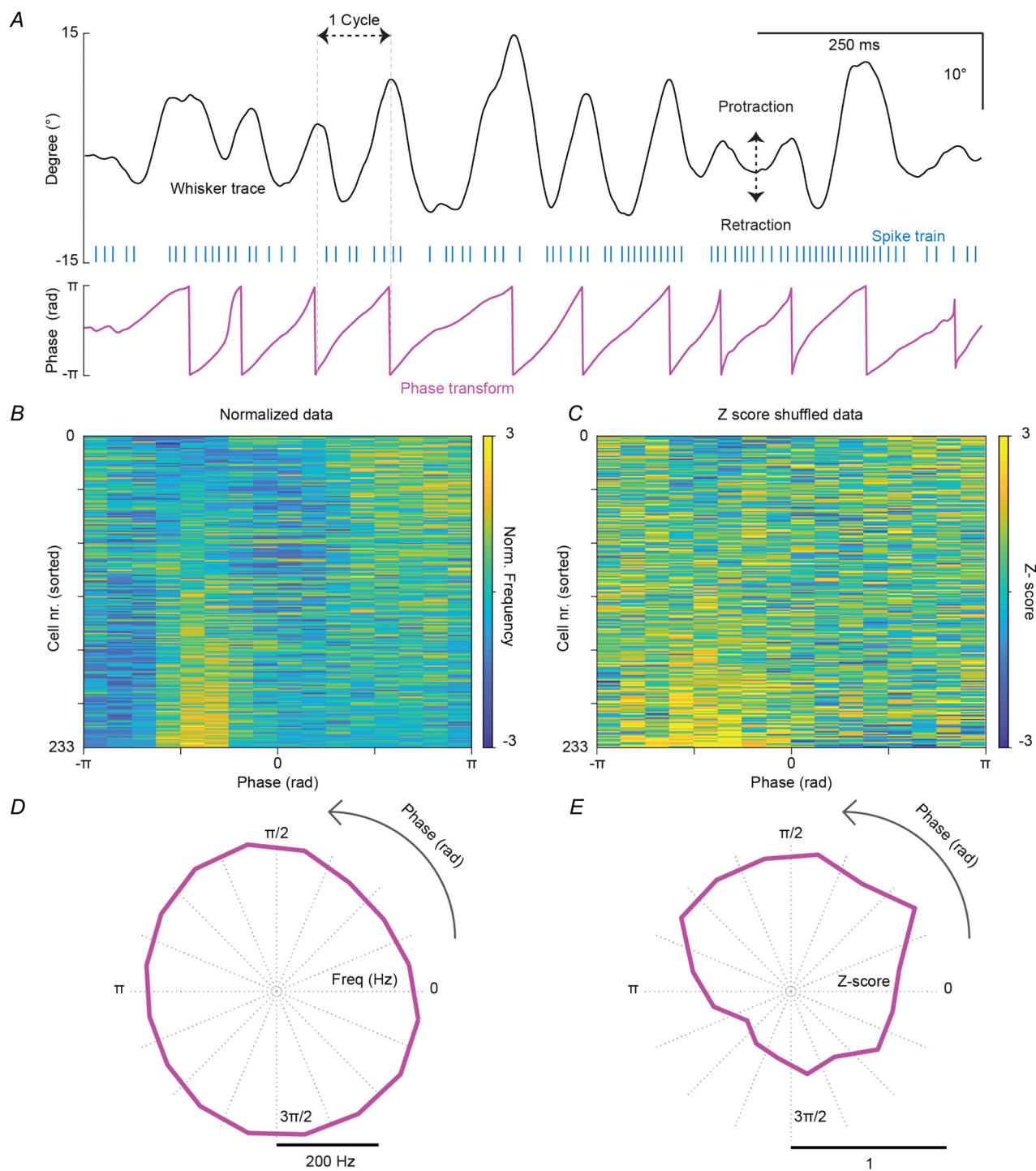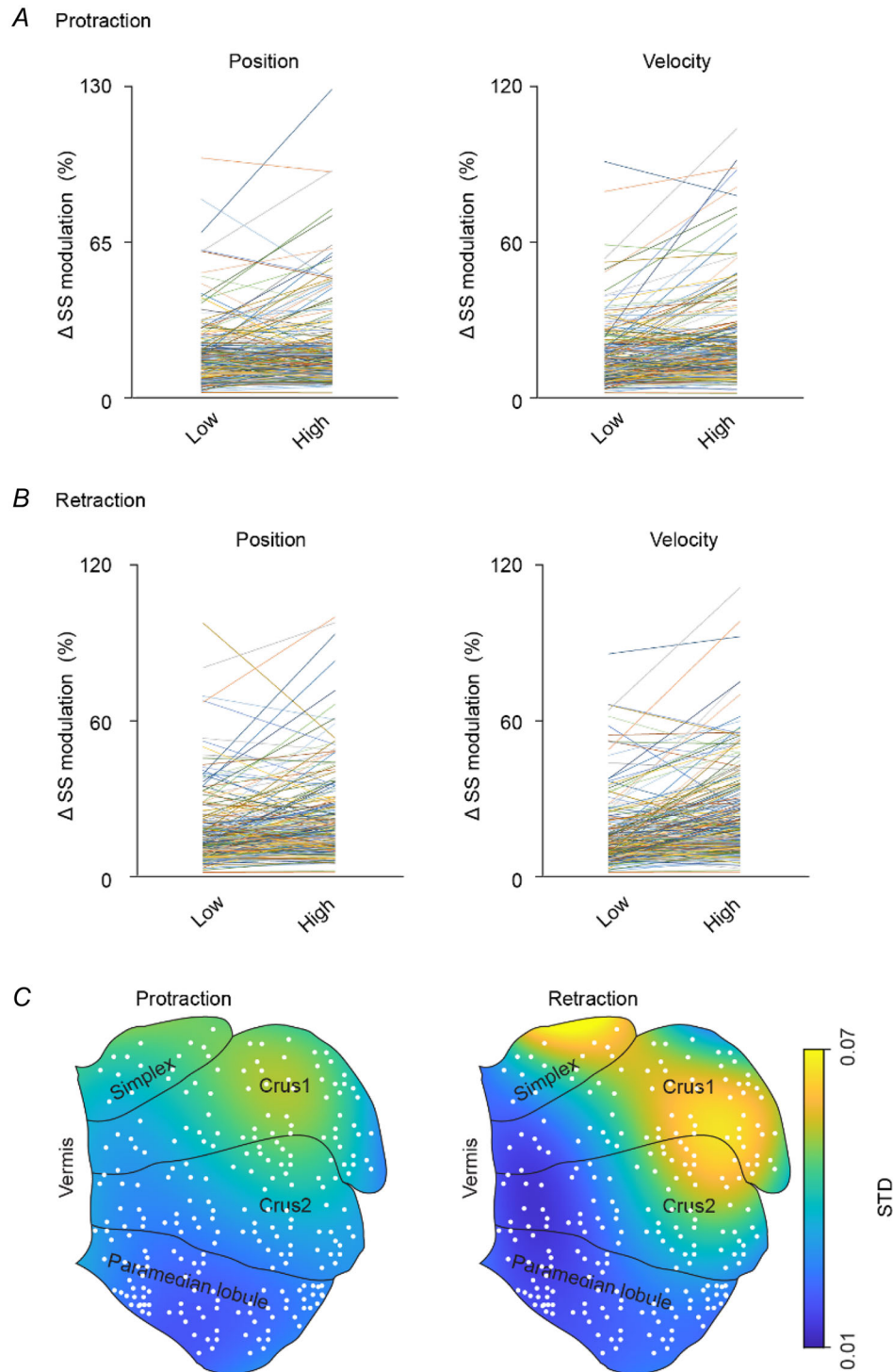
Figure A3.
SS modulation in the phase domain. *A*, example of a whisker trace (top panel, black), with a spike train (middle, blue) and the whisker Hilbert phase transform (bottom, pink). *B*, normalized simple spike activity during the phase progression of the whisking cycle. In the heatmap, each row represents the SS activity of each PC. Columns depict the phase of the whisker cycle, split into 16 bins. *C*, heatmap showing the Z-scores of the real data compared to randomly permutated simple spikes (100 random permutations). The fact that the Z-score appears less modulated than the SS count per bin in *C* indicates that unequal distribution of SSs during the whisking cycle can be obtained also after random shuffling of SSs. *D*, circular plot showing the mean firing rate from *B* during each phase of whisking. The centre is 0 Hz and the bar indicates the distance from the centre which is 200 Hz. *E*, circular plot showing the mean Z-scores from the heatmap in *C*. The centre is a Z-score of 0 and the bar indicates the distance from the centre to a Z-score of 1.

Figure A4.

Weak CS modulation during different phases of whisker movements. *A*, example of a whisker movement trace and the protraction and retraction segments. *B*, enlargement of subsequent protraction and retraction segments and the relative morphological parameters (i.e. amplitude and duration). Note whisker movement segments with different starting and ending points can have the same amplitude and protraction and retraction segments of the same cycle can have different amplitudes (position at the end-point minus position of the starting-point). The velocity of each segment was calculated by dividing the amplitude by the duration. *C*, examples of cells (same cells for which SSs are shown in Fig. 3*B*) of CS firing rate around the four reference points of the whisker movements. The dark and light orange lines, as well as the dark and light blues, represent the CS modulation at the start of protraction, the end of protraction, the start of retraction and the end of retraction, respectively. *D*, heatmap of CS modulation for all 233 PCs when aligned at the start of protraction (top), end of protraction (top-middle), start of

retraction (bottom-middle) and end of retraction (bottom). Each row represents the CS modulation of one cell. The rows are sorted according to the maximal modulation for the first 50 ms after the start of the respective whisker movement. Note the relatively weak correlations.
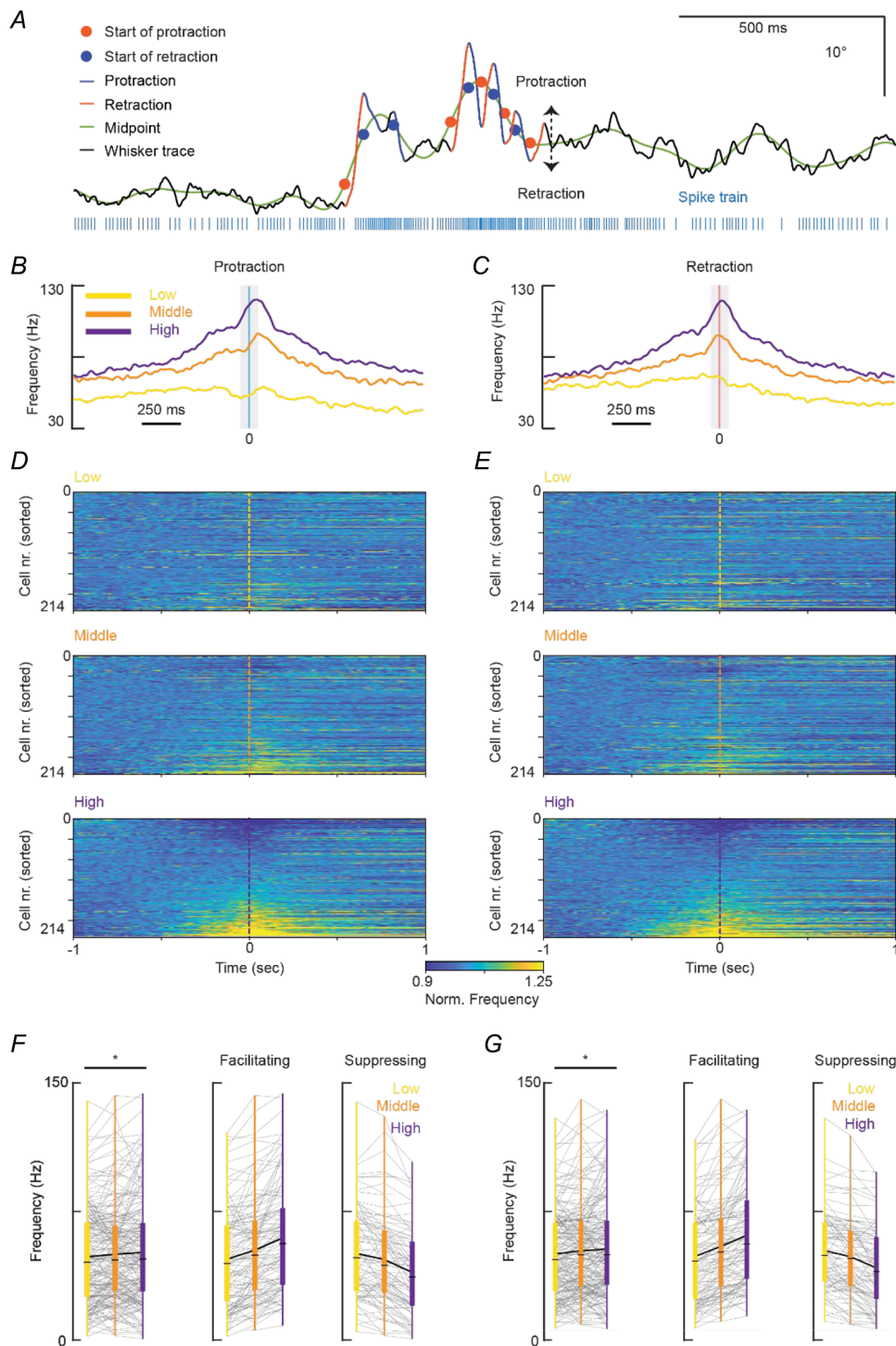

Figure A5.
SS correlation with individual whisker movement for each PC. *A*, the values of ΔSS rate summarized in the bar plots of Fig. 4C are shown for individual cells. Each line represents the mean ΔSS rate of one individual PC for protractions with 'low' and 'high' amplitude (left) or 'low' and 'high' velocity (right). *B*, similar to *A*, but for

retraction. *C*, variability relative to the heatmap of Fig. *4F* is shown for each region of the cerebellar hemisphere. Colour indicates the standard deviation of the R^2 of linear correlation between the velocity of individual whisker protraction and SS (top) or CS (bottom) rate. Each white dot represents the approximate location where each PC was recorded.
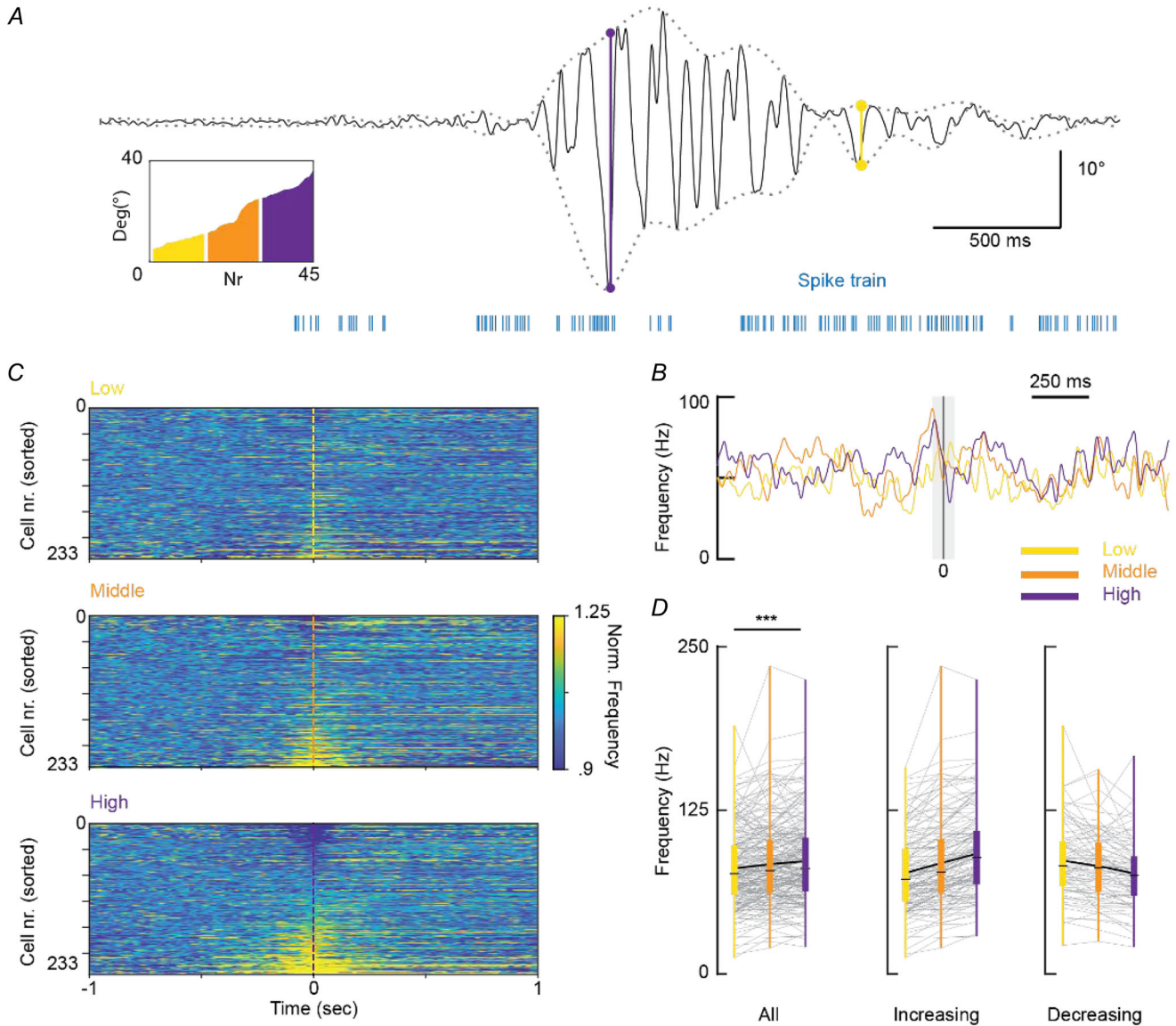
Figure A6.

Simple spike modulation around peak values in the envelope. *A*, example of a whisker movement as a raw trace (top panel, black), together with the envelope (top panel, dotted line). Peaks in envelope value (upper envelope minus lower envelope) are highlighted with two dots on the dotted line, connected with a vertical line. Envelope peaks are classified into three equal groups. Inset shows the distribution of groups from exemplary cell. The blue spike train (lower panel) indicates the simple spikes during the whisker trace from the upper panel. *B*, convolved peri-event time histogram (PETH) of SS firing rate around the peak in the envelope from an exemplary cell from *A*. The three equal groups with a low, middle or high envelope are highlighted in yellow, orange and purple, respectively. The shaded area indicates the time window used for further analyses. *C*, convolved and normalized PETH for the whole population of 233 cells, shown as a heatmap where each row represents one cell, classified as low, middle or high. Cells are sorted for the maximum modulation from −50 to 250 ms relative to the onset of protraction from the 'high' group. *D*, boxplot showing the modulation extracted from the convolved PETH per group as the mean from −50 to 50 ms relative to the onset of protraction. On the left are all PCs shown together ($P = 1.45 \times 10^{-6}$, paired *t* test). On the middle and right the PCs are separated based on either an increase or decrease of their maximum value in the high group compared to the low group.
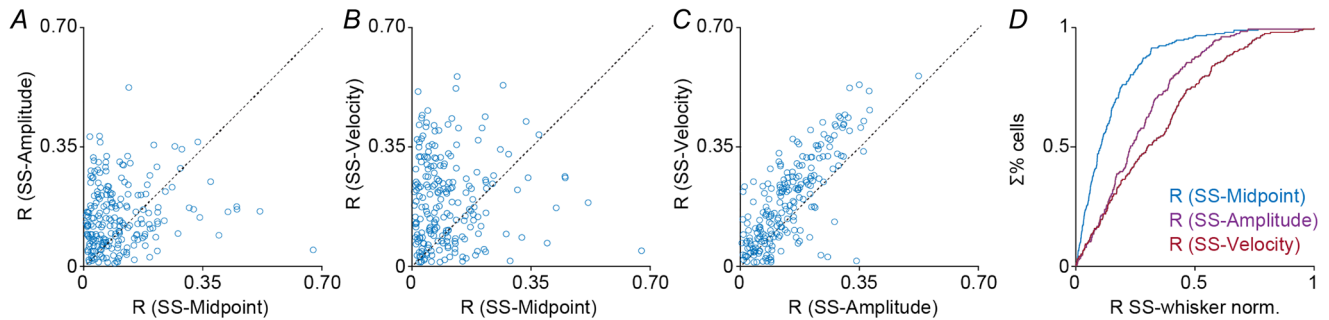
Figure A7.

Simple spike modulation of protraction and retraction varies with the midpoint. *A*, example of a whisker movement as a raw trace (top panel, black), and together with the midpoint (calculated as the 6 Hz low-pass filtered whisker trace, top panel, green). Spontaneous whisker movements are characterized by quasiperiodic oscillations consisting of protractions and retractions, highlighted in orange and blue, respectively. The starting point is highlighted by the dots in a similar colour on the midpoint. The blue spike train (lower panel) indicates the simple spikes during the whisker trace from the upper panel. *B*, convolved peri-event time histogram (PETH) of SS firing rate around the start of a protraction for exemplary cell from *A*. Protractions are sorted for the midpoint value at the start of the protraction and classified into three equal groups with a low, middle or high midpoint, highlighted in yellow, orange and purple, respectively. The shaded area indicates the time window used for further analyses. *C*, similar to

B but for retractions of the exemplary cell. *D*, convolved and normalized PETH for the 214 cells for which changes in the midpoint were detected, shown as a heatmap where each row represents one cell, classified as low, middle or high. Cells are sorted for the maximum modulation from −250 to 250 ms relative to the onset of protraction from the 'high' group. *E*, similar to *D* but for retraction. *F*, boxplot showing the modulation extracted from the convolved PETH per group as the maximum from −50 to 50 ms relative to the onset of protraction. On the left, all PCs are shown together ($P = 0.032$, paired *t* test). In the middle and on the right, the PCs that either increase or decrease their maximum SS rate in the high group compared to the low group are shown separately. *G*, similar to *F* but for retraction ($P = 0.0056$, paired *t* test).
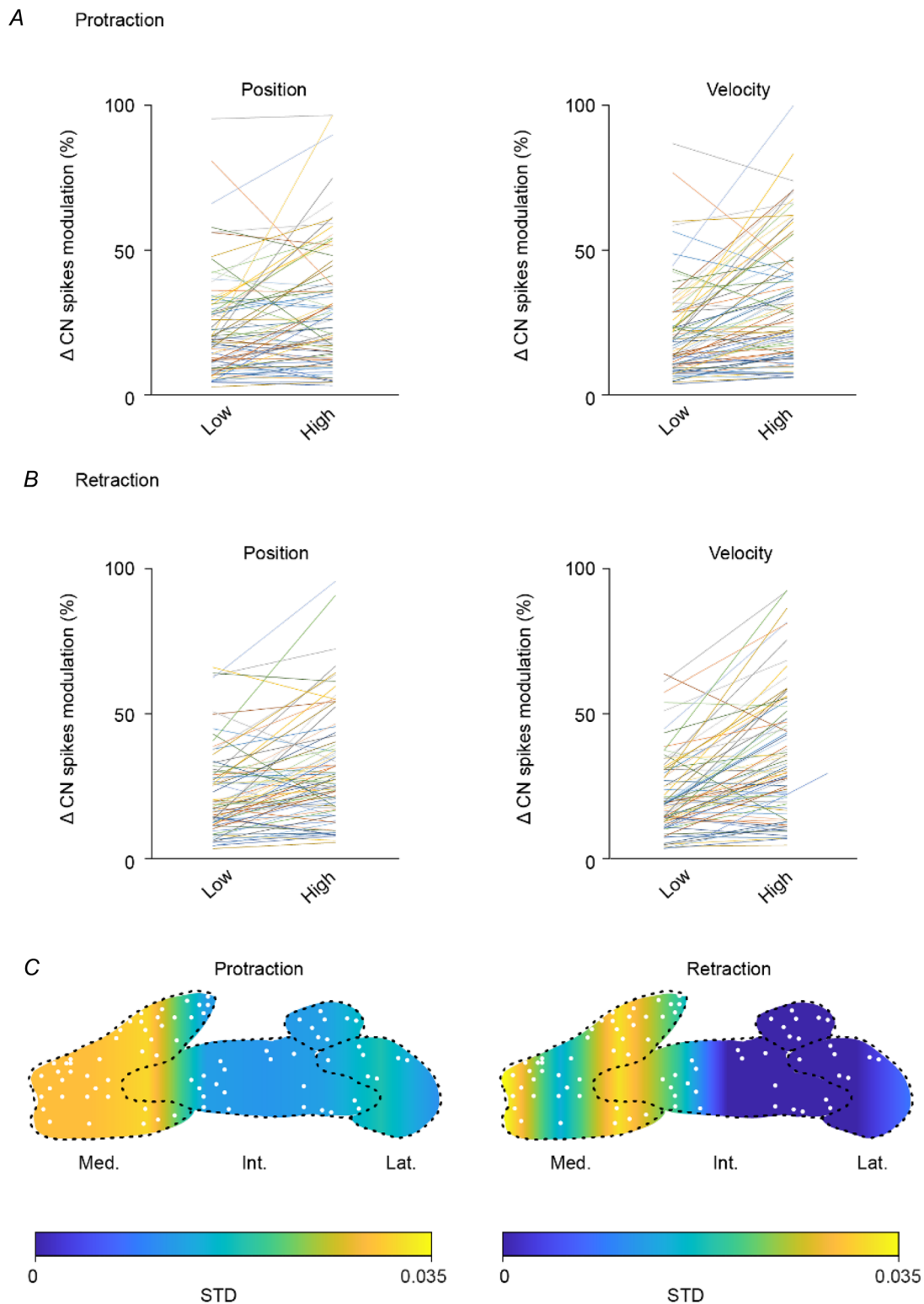

Figure A8.

The PCs correlating with the midpoint are different from the PCs correlating with the amplitude and velocity of the individual segments. *A*, the *R* values of the linear fitting between SS rate and midpoint or individual protraction amplitude are compared with a scatterplot. The lack of correlation (Pearson $r = 0.12$, $P = 0.09$) indicates that the PCs for which the SS rate correlates well with the midpoint are different from those that correlate well with the amplitude of the individual protractions. *B*, same as *A*, but for correlation midpoint and velocity of the individual protractions (Pearson $r = 0.03$, $P = 0.63$). *C*, conversely, PCs for which SS rate correlated well with the amplitude of the individual protractions are the same that correlate well with the velocity of the individual protractions (Pearson $r = 0.77$, $P = 2.52 \times 10^{-44}$). The fact that the large majority of dots are above the diagonal indicates that the SS correlation with the velocity is higher than for amplitude ($P = 5.22 \times 10^{-5}$, paired *t* test). *D*, the normalized cumulative distribution function of the midpoint, amplitude and velocity correlation with SS.
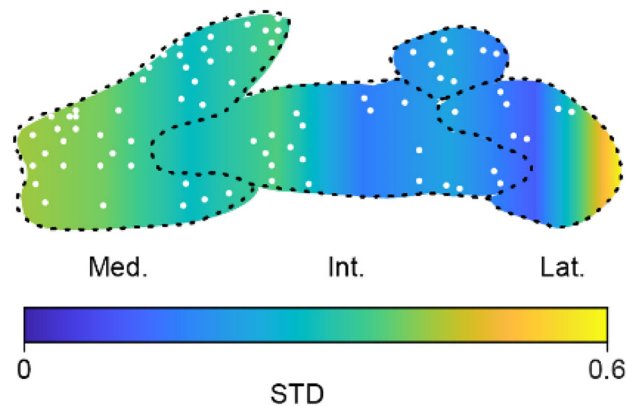
Figure A9.

Variability relative to the heatmap of Fig. 5*E* is shown for each region of the cerebellar nuclei. The colour code indicates the standard deviation of the change in whisker position associated with CN spike rate. Each white dot represents the approximate location where each putative CN neuron was recorded.

Figure A10.
CN spike correlation with individual whisker movement for each putative CN neuron. *A*, the values of ΔSS rate summarized in the bar plots of Fig. 4*C* are shown for each individual cell. Each line represents the mean CN spike rate of one individual CN neuron for protractions with 'low' and 'high' amplitude (left) or 'low' and 'high' velocity (right). *B*, similar to *A*, but for retraction. *C*, the variability relative to the heatmap of Fig. 6*F* is shown for each region of the cerebellar nuclei. The colour indicates the standard deviation of the R^2 of linear correlation between the velocity of individual whisker protraction and CN spike rate. Each white dot represents the approximate location where each putative CN neuron was recorded.

© 2023 The Authors. *The Journal of Physiology* published by John Wiley & Sons Ltd on behalf of The Physiological Society.

References

Apps, R., & Hawkes, R.(2009). Cerebellar cortical organization: A one-map hypothesis. *Nature Reviews Neuroscience*, **10**(9), 670–681.

Apps, R., Hawkes, R., Aoki, S., Bengtsson, F., Brown, A. M., Chen, G., Ebner, T. J., Isope, P., Jörntell, H., Lackey, E. P., Lawrenson, C., Lumb, B., Schonewille, M., Sillitoe, R. V., Spaeth, L., Sugihara, I., Valera, A., Voogd, J., Wylie, D. R., & Ruigrok, T. J. H.(2018). Correction to: Cerebellar modules and their role as operational cerebellar processing units: A consensus paper. *Cerebellum (London, England)*, **17**(5), 683–684.

Apps, R., & Lidierth, M.(1989). Simple spike discharge patterns of Purkinje cells in the paramedian lobule of the cerebellum during locomotion in the awake cat. *Neuroscience Letters*, **102**(2–3), 205–210.

Auffret, M., Ravano, V. L., Rossi, G. M. C., Hankov, N., Petersen, M. F. A., & Petersen, C. C. H.(2018). Optogenetic stimulation of cortex to map evoked whisker movements in awake head-restrained mice. *Neuroscience*, **368**, 199–213.

Bauer, S., Van Wingerden, N., Jacobs, T., Van Der Horst, A., Zhai, P., Betting, J.-H. L. F., Strydis, C., White, J. J., De Zeeuw, C. I., & Romano, V.(2022). Purkinje cell activity resonation generates rhythmic behaviors at the preferred frequency of 8 Hz. *Biomedicines*, **10**(8), 1831.

Beekhof, G. C., Gornati, S. V., Canto, C. B., Libster, A. M., Schonewille, M., De Zeeuw, C. I., & Hoebeek, F. E.(2021). Activity of cerebellar nuclei neurons correlates with Zebrinii identity of their Purkinje cell afferents. *Cells-Basel*, **10**(10), 2686.

Bellavance, M.-A., Takatoh, J., Lu, J., Demers, M., Kleinfeld, D., Wang, F., & Deschênes, M.(2017). Parallel inhibitory and excitatory trigemino-facial feedback circuitry for reflexive vibrissa movement. *Neuron*, **95**(3), 722–723.

Bermejo, R., Friedman, W., & Zeigler, H. P.(2005). Topography of whisking II: Interaction of whisker and pad. *Somatosensory & Motor Research*, **22**(3), 213–220.

Bina, L., Romano, V., Hoogland, T. M., Bosman, L. W. J., & De Zeeuw, C. I.(2021). Purkinje cells translate subjective salience into readiness to act and choice performance. *Cell Reports*, **37**(11), 110116.

Bosman, L. W. J., Houweling, A. R., Owens, C. B., Tanke, N., Shevchouk, O. T., Rahmati, N., Teunissen, W. H. T., Ju, C., Gong, W., Koekkoek, S. K. E., & De Zeeuw, C. I.(2011). Anatomical pathways involved in generating and sensing rhythmic whisker movements. *Frontiers in Integrative Neuroscience*, **5**, 53.

Bosman, L. W. J., Koekkoek, S. K. E., Shapiro, J., Rijken, B. F. M., Zandstra, F., Van Der Ende, B., Owens, C. B., Potters, J.-W., De Gruijl, J. R., Ruigrok, T. J. H., & De Zeeuw, C. I.(2010). Encoding of whisker input by cerebellar Purkinje cells. *The Journal of Physiology*, **588**(19), 3757–3783.

Brooks, J. X., Carriot, J., & Cullen, K. E.(2015). Learning to expect the unexpected: rapid updating in primate cerebellum during voluntary self-motion. *Nature Neuroscience*, **18**(9), 1310–1317.

Brown, S. T., & Raman, I. M.(2018). Sensorimotor integration and amplification of reflexive whisking by well-timed spiking in the cerebellar corticonuclear circuit. *Neuron*, **99**(3), 564–575.e2.

Cao, Y., Roy, S., Sachdev, R. N. S., & Heck, D. H.(2012). Dynamic correlation between whisking and breathing rhythms in mice. *Journal of Neuroscience*, **32**(5), 1653–1659.

Chaumont, J., Guyon, N., Valera, A. M., Dugué, G. P., Popa, D., Marcaggi, P., Gautheron, V., Reibel-Foisset, S., Dieudonné, S., Stephan, A., Barrot, M., Cassel, J.-C., Dupont, J.-L., Doussau, F., Poulain, B., Selimi, F., Léna, C., & Isope, P.(2013). Clusters of cerebellar Purkinje cells control their afferent climbing fiber discharge. *Proceedings of the National Academy of Sciences*, **110**(40), 16223–16228.

Chen, S., Augustine, G. J., & Chadderton, P.(2016). The cerebellum linearly encodes whisker position during voluntary movement. *Elife*, **5**, e10509.

Cheung, J., Maire, P., Kim, J., Sy, J., & Hires, S. A.(2019). The sensorimotor basis of whisker-guided anteroposterior object localization in head-fixed mice. *Current Biology*, **29**(18), 3029–3040.e4.

Crochet, S., Poulet, J. F. A., Kremer, Y., & Petersen, C. C. H.(2011). Synaptic mechanisms underlying sparse coding of active touch. *Neuron*, **69**(6), 1160–1175.

De Gruijl, J. R., Hoogland, T. M., & De Zeeuw, C. I.(2014). Behavioral correlates of complex spike synchrony in cerebellar microzones. *Journal of Neuroscience*, **34**(27), 8937–8947.

De Zeeuw, C. I.(2021). Bidirectional learning in upbound and downbound microzones of the cerebellum. *Nature Reviews Neuroscience*, **22**(2), 92–110.

De Zeeuw, C. I., & Berrebi, A. S.(1995). Postsynaptic targets of Purkinje cell terminals in the cerebellar and vestibular nuclei of the rat. *European Journal of Neuroscience*, **7**(11), 2322–2333.

De Zeeuw, C. I., Hoebeek, F. E., Bosman, L. W. J., Schonewille, M., Witter, L., & Koekkoek, S. K.(2011). Spatiotemporal firing patterns in the cerebellum. *Nature Reviews Neuroscience*, **12**(6), 327–344.

De Zeeuw, C. I., Wylie, D. R., Stahl, J. S., & Simpson, J. I.(1995). Phase relations of Purkinje cells in the rabbit flocculus during compensatory eye movements. *Journal of Neurophysiology*, **74**(5), 2051–2064.

Ebner, T. J., Hewitt, A. L., & Popa, L. S.(2011). What features of limb movements are encoded in the discharge of cerebellar neurons? *Cerebellum (London, England)*, **10**(4), 683–693.

Hattox, A. M., Priest, C. A., & Keller, A.(2002). Functional circuitry involved in the regulation of whisker movements. *Journal of Comparative Neurology*, **442**(3), 266–276.

Heffley, W., & Hull, C.(2019). Classical conditioning drives learned reward prediction signals in climbing fibers across the lateral cerebellum. *Elife*, **8**, e46764.

Heiney, S. A., Kim, J., Augustine, G. J., & Medina, J. F.(2014). Precise control of movement kinematics by optogenetic inhibition of Purkinje cell activity. *Journal of Neuroscience*, **34**(6), 2321–2330.

Heiney, S. A., Wohl, M. P., Chettih, S. N., Ruffolo, L. I., & Medina, J. F.(2014). Cerebellar-dependent expression of motor learning during eyeblink conditioning in head-fixed mice. *Journal of Neuroscience*, **34**(45), 14845–14853.

Heiney, S. A., Wojaczynski, G. J., & Medina, J. F.(2021). Action-based organization of a cerebellar module specialized for predictive control of multiple body parts. *Neuron*, **109**(18), 2981–2994.e5.

Herzfeld, D. J., Kojima, Y., Soetedjo, R., & Shadmehr, R.(2015). Encoding of action by the Purkinje cells of the cerebellum. *Nature*, **526**(7573), 439–442.

Hewitt, A. L., Popa, L. S., Pasalar, S., Hendrix, C. M., & Ebner, T. J.(2011). Representation of limb kinematics in Purkinje cell simple spike discharge is conserved across multiple tasks. *Journal of Neurophysiology*, **106**(5), 2232–2247.

Hill, D. N., Bermejo, R., Zeigler, H. P., & Kleinfeld, D.(2008). Biomechanics of the vibrissa motor plant in rat: Rhythmic whisking consists of triphasic neuromuscular activity. *Journal of Neuroscience*, **28**(13), 3438–3455.

Hill, D. N., Curtis, J. C., Moore, J. D., & Kleinfeld, D.(2011). Primary motor cortex reports efferent control of vibrissa motion on multiple timescales. *Neuron*, **72**(2), 344–356.

Hoogland, T. M., De Gruijl, J. R., Witter, L., Canto, C. B., & De Zeeuw, C. I. (2015). Role of synchronous activation of cerebellar purkinje cell ensembles in multi-joint movement control. *Current Biology*, **25**(9), 1157–1165.

Kleinfeld, D., Ahissar, E., & Diamond, M. E.(2006). Active sensation: insights from the rodent vibrissa sensori-motor system. *Current Opinion in Neurobiology*, **16**(4), 435–444.

Kleinfeld, D., Deschênes, M., & Ulanovsky, N.(2016). Whisking, sniffing, and the hippocampal theta-rhythm: A tale of two oscillators. *PLoS Biology*, **14**(2), e1002385.

Kostadinov, D., Beau, M., Blanco-Pozo, M., & Häusser, M.(2019). Predictive and reactive reward signals conveyed by climbing fiber inputs to cerebellar Purkinje cells. *Nature Neuroscience*, **22**(6), 950–962.

Lang, E. J., Sugihara, I., & Llinás, R.(2006). Olivocerebellar modulation of motor cortex ability to generate vibrissal movements in rat. *The Journal of Physiology*, **571**(1), 101–120.

Lindeman, S., Hong, S., Kros, L., Mejias, J. F., Romano, V., Oostenveld, R., Negrello, M., Bosman, L. W. J., & De Zeeuw, C. I.(2021). Cerebellar Purkinje cells can differentially modulate coherence between sensory and motor cortex depending on region and behavior. *Proceedings of the National Academy of Sciences*, **118**(2),

Marple-Horvat, D. E., & Stein, J. F.(1990). Neuronal activity in the lateral cerebellum of trained monkeys, related to visual stimuli or to eye movements. *The Journal of Physiology*, **428**(1), 595–614.

Miall, R. C., Keating, J. G., Malkmus, M., & Thach, W. T.(1998). Simple spike activity predicts occurrence of complex spikes in cerebellar Purkinje cells. *Nature Neuroscience*, **1**(1), 13–15.

Moore, J. D., Deschênes, M., Furuta, T., Huber, D., Smear, M. C., Demers, M., & Kleinfeld, D.(2013). Hierarchy of orofacial rhythms revealed through whisking and breathing. *Nature*, **497**(7448), 205–210.

Muzzu, T., Mitolo, S., Gava, G. P., & Schultz, S. R.(2018). Encoding of locomotion kinematics in the mouse cerebellum. *PLoS ONE*, **13**(9), e0203900.

O'connor, S. M., Berg, R. W., & Kleinfeld, D.(2002). Coherent electrical activity between vibrissa sensory areas of cerebellum and neocortex is enhanced during free whisking. *Journal of Neurophysiology*, **87**(4), 2137–2148.

Pellerin, J.-P., & Lamarre, Y.(1997). Local field potential oscillations in primate cerebellar cortex during voluntary movement. *Journal of Neurophysiology*, **78**(6), 3502–3507.

Perkon, I., Košir, A., Itskov, P. M., Tasič, J., & Diamond, M. E.(2011). Unsupervised quantification of whisking and head movement in freely moving rodents. *Journal of Neurophysiology*, **105**(4), 1950–1962.

Person, A. L., & Raman, I. M.(2011). Purkinje neuron synchrony elicits time-locked spiking in the cerebellar nuclei. *Nature*, **481**(7382), 502–505.

Person, A. L., & Raman, I. M.(2012). Synchrony and neural coding in cerebellar circuits. *Front Neural Circuits*, **6**, 97.

Prescott, T. J., Diamond, M. E., & Wing, A. M.(2011). Active touch sensing. *Philosophical Transactions of the Royal Society of London. Series B: Biological Sciences*, **366**(1581), 2989–2995.

Proville, R. D., Spolidoro, M., Guyon, N., Dugué, G. P., Selimi, F., Isope, P., Popa, D., & Léna, C.(2014). Cerebellum involvement in cortical sensorimotor circuits for the control of voluntary movements. *Nature Neuroscience*, **17**(9), 1233–1239.

Romano, V., De Propris, L., Bosman, L. W.j, Warnaar, P., Ten Brinke, M. M., Lindeman, S., Ju, C., Velauthapillai, A., Spanke, J. K., Middendorp Guerra, E., Hoogland, T. M., Negrello, M., D'angelo, E., & De Zeeuw, C. I.(2018). Potentiation of cerebellar Purkinje cells facilitates whisker reflex adaptation through increased simple spike activity. *Elife*, **7**, e38852.

Romano, V., Reddington, A. L., Cazzanelli, S., Mazza, R., Ma, Y., Strydis, C., Negrello, M., Bosman, L. W. J., & De Zeeuw, C. I.(2020). Functional convergence of autonomic and sensorimotor processing in the lateral cerebellum. *Cell reports*, **32**(1), 107867.

Romano, V., Zhai, P., Van Der Horst, A., Mazza, R., Jacobs, T., Bauer, S., Wang, X., White, J. J., & De Zeeuw, C. I.(2022). Olivocerebellar control of movement symmetry. *Current Biology*, **32**(3), 654–670.e4.

Sauerbrei, B. A., Lubenov, E. V., & Siapas, A. G.(2015). Structured variability in purkinje cell activity during locomotion. *Neuron*, **87**(4), 840–852.

Schreurs, B. G., Anchez-Andres, J. V., & Alkon, D. L.(1991). Learning-specific differences in Purkinje-cell dendrites of lobule HVI (Lobulus simplex): intracellular recording in a rabbit cerebellar slice. *Brain Research*, **548**(1–2), 18–22.

Sedaghat-Nejad, E., Pi, J. S., Hage, P., Fakharian, M. A., & Shadmehr, R.(2022). Synchronous spiking of cerebellar Purkinje cells during control of movements. *Proceedings of the National Academy of Sciences*, **119**(14), e2118954119.

Shambes, G. M., Gibson, J. M., & Welker, W.(1978). Fractured somatotopy in granule cell tactile areas of rat cerebellar hemispheres revealed by micromapping. *Brain Behavior and Evolution* **15**(2), 94–105.

Sharp, F. R., & Gonzalez, M. F.(1985). Multiple vibrissae sensory regions in rat cerebellum: A (14C) 2-deoxyglucose study. *Journal of Comparative Neurology*, **234**(4), 489–500.

Sharp, F. R., Gonzalez, M. F., Sharp, J. W., & Sagar, S. M.(1989). c-fos expression and (14C) 2-deoxyglucose uptake in the caudal cerebellum of the rat during motor/sensory cortex stimulation. *Journal of Comparative Neurology*, **284**(4), 621–636.

Sreenivasan, V., Esmaeili, V., Kiritani, T., Galan, K., Crochet, S., & Petersen, C. C. H.(2016). Movement initiation signals in mouse whisker motor cortex. *Neuron*, **92**(6), 1368–1382.

Sugihara, I., Fujita, H., Na, J., Quy, P. N., Li, B.-Y., & Ikeda, D.(2009). Projection of reconstructed single Purkinje cell axons in relation to the cortical and nuclear aldolase C compartments of the rat cerebellum. *Journal of Comparative Neurology*, **512**(2), 282–304.

Takatoh, J., Prevosto, V., Thompson, P. M., Lu, J., Chung, L., Harrahill, A., Li, S., Zhao, S., He, Z., Golomb, D., Kleinfeld, D., & Wang, F.(2022). The whisking oscillator circuit. *Nature*, **609**(7927), 560–568.

Ten Brinke, M. M., Boele, H.-J., Spanke, J. K., Potters, J.-W., Kornysheva, K., Wulff, P., Ijpelaar, A. C. H. G., Koekkoek, S. K. E., & De Zeeuw, C. I.(2015). Evolving models of pavlovian conditioning: Cerebellar cortical dynamics in awake behaving mice. *Cell reports*, **13**(9), 1977–1988.

Teune, T. M., van der Burg, J., van der Moer, J., Voogd, J., & Ruigrok, T. J.(2000). Topography of cerebellar nuclear projections to the brain stem in the rat. *Progress in Brain Research*, **124**, 141–172.

Thach, W. T.(1968). Discharge of Purkinje and cerebellar nuclear neurons during rapidly alternating arm movements in the monkey. *Journal of Neurophysiology*, **31**(5), 785–797.

Towal, R. B., & Hartmann, M. J. Z.(2008). Variability in velocity profiles during free-air whisking behavior of unrestrained rats. *Journal of Neurophysiology*, **100**(2), 740–752.

Voges, K., Wu, B., Post, L., Schonewille, M., & De Zeeuw, C. I.(2017). Mechanisms underlying vestibulo-cerebellar motor learning in mice depend on movement direction. *The Journal of Physiology*, **595**(15), 5301–5326.

Wagner, M. J., Savall, J., Hernandez, O., Mel, G., Inan, H., Rumyantsev, O., Lecoq, J., Kim, T. H., Li, J. Z., Ramakrishnan, C., Deisseroth, K., Luo, L., Ganguli, S., & Schnitzer, M. J.(2021). A neural circuit state change underlying skilled movements. *Cell*, **184**(14), 3731–3747.e21.

Wang, X., Yu, S.i-Y., Ren, Z., De Zeeuw, C. I., & Gao, Z.(2020). A FN-MdV pathway and its role in cerebellar multimodular control of sensorimotor behavior. *Nature Communications*, **11**(1), 6050.

White, J. J., & Sillitoe, R. V.(2017). Genetic silencing of olivocerebellar synapses causes dystonia-like behaviour in mice. *Nature Communications*, **8**(1), 14912.

Wineski, L. E.(1983). Movements of the Cranial Vibrissae in the Golden-Hamster (Mesocricetus-Auratus). *Journal of Zoology*, **200**(2), 261–280.

Witter, L., Canto, C. B., Hoogland, T. M., De Gruijl, J. R., & De Zeeuw, C. I.(2013). Strength and timing of motor responses mediated by rebound firing in the cerebellar nuclei after Purkinje cell activation. *Front Neural Circuits*, **7**, 133.

Additional information

Data availability statement

All data are available from the Lead Contact upon request. The data used for this paper are also available for reuse on a public repository: 'Simple and complex spikes of cerebellar Purkinje cells and simultaneously tracked whisker voluntary movement'; Romano, V., Zhai, P., & De Zeeuw, C. I. (2022); EBRAINS https://doi.org/10.25493/42NK-RYF.

The custom code complementing BWTT whisker tracking can be obtained via https://github.com/elifesciences-publications/BWTT_PP.

Competing interests

The authors have no financial, professional or personal conflicts relating to this publication.

Author contributions

P.Z., C.I.D.Z. and V.R. designed the experiments. P.Z., G.S., R.M. and V.R. performed the experiments. P.Z., G.S., R.M., S.B., N.v.W., A.v.d.H., T.J. and V.R. analysed the data and contributed to data visualization. P.Z., C.I.D.Z., V.R., S.B. and J.J.W wrote and revised the article.

Keywords

cerebellar hemisphere, cerebellar nuclei, complex spikes, crus1, crus2, lobule simplex, paramedian lobule, simple spikes

Supporting information

Additional supporting information can be found online in the Supporting Information section at the end of the HTML view of the article. Supporting information files available:

Statistical Summary Document
Peer Review History